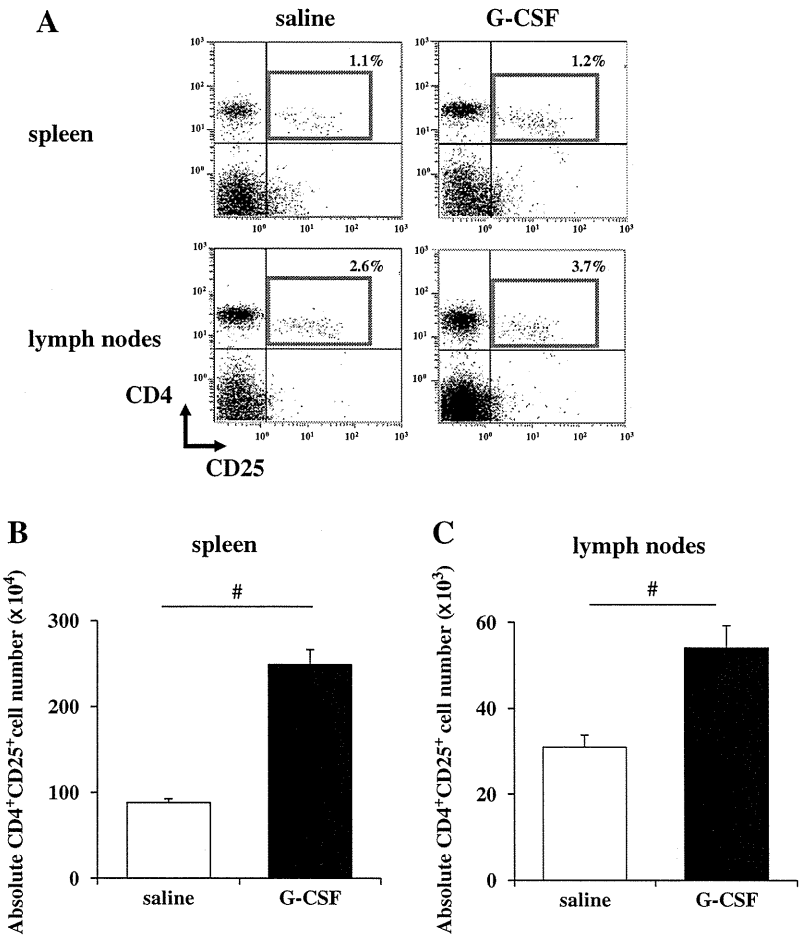

Fig. 4. Effects of G-CSF on the total cell number of Tregs in spleen and inguinal lymph nodes. (A) The proportions of $CD4^+CD25^+$ Tregs from the G-CSF- or the saline-treated mice assessed by flow cytometric analysis. The total cell number of $CD4^+CD25^+$ Tregs was counted in spleen (B) and inguinal lymph nodes (C) after G-CSF treatment. $^*P<0.05$. $\#P<0.01$. The means ± SEM of 6 animals are shown.

mice compared with the saline-treated mice (G-CSF group: 8.7 ± 4.9 cells/mm^2 vs. saline group: 2.8 ± 3.6 cells/mm^2, $P<0.05$) (Fig. 5B).

3.5. Involvement of Tregs in G-CSF-induced atheroprotective effects

To confirm whether Tregs were involved in mechanisms of the atheroprotective effects of G-CSF, we examined the effects of G-CSF on Tregs-depleted $ApoE^{-/-}$ mice using PC61. More than 90% of $CD4^+CD25^+$ Tregs were decreased in inguinal lymph nodes at 14 days after a single intraperitoneal injection of 100 μg of PC61 (Fig. 6A). Administration of this antibody every two weeks abolished the protective effects of G-CSF on atherosclerosis. G-CSF significantly reduced the area of Oil Red-O-positive atherosclerotic lesion in $ApoE^{-/-}$ mice, but the Oil Red-O-positive atherosclerotic lesion area was not significantly different between the saline-treated Tregs-depleted $ApoE^{-/-}$ mice (PC61-saline group) and the G-CSF-treated Tregs-depleted $ApoE^{-/-}$ mice (PC61-G-CSF group) (PC61-G-CSF group: $18.0 \pm 2.6 \times 10^4$ μm^2 vs. PC61-saline group: $18.8 \pm 2.3 \times 10^4$ μm^2, $P=0.67$) (Fig. 6B, C). G-CSF significantly reduced the level of IFN-γ and increased the level of IL-10 in $ApoE^{-/-}$ mice, but the levels of IFN-γ and IL-10 also were not different between the PC61-saline group and the PC61-G-CSF group (IFN-γ; PC61-G-CSF group: 37.1 ± 8.0% vs. PC61-saline group: 38.2 ± 8.5%, $P=0.82$, IL-10; PC61-G-CSF group: 5.1 ± 2.6% vs. PC61-saline group: 5.8 ± 1.3%, $P=0.62$) (Fig. 6D, E).

Furthermore, we examined the effects of G-CSF on atherosclerosis using $ApoE^{-/-}/CD28^{-/-}$ double knockout (DKO) mice. In the DKO mice, approximately 90% of $CD4^+CD25^+$ Tregs were decreased in inguinal lymph nodes (Fig. 7A). The treatment with G-CSF did not reduce the atherosclerotic lesion area in the DKO mice (G-CSF group: $17.8 \pm 0.9 \times 10^4$ μm^2 vs. saline group: $17.5 \pm 1.8 \times 10^4$ μm^2, $P=0.67$) (Fig. 7B). The levels of IFN-γ and IL-10 were not different between the saline group and the G-CSF group (IFN-γ; G-CSF group: 31.3 ± 3.8% vs. saline group: 31.3 ± 1.5%, $P=0.99$, IL-10; G-CSF group: 6.3 ± 0.5% vs. saline group: 6.2 ± 0.9%, $P=0.86$) (Fig. 7C, D).

4. Discussion

In the present study, we demonstrated that G-CSF prevents the progression of atherosclerosis and that the increased Tregs subset is involved in the atheroprotective mechanism of G-CSF in $ApoE^{-/-}$ mice. Interestingly, the blood lipid concentrations were not significantly different between the G-CSF-treated mice and the saline-treated mice. G-CSF increased the number of Foxp3-positive Tregs in atherosclerotic lesions, along with the decreased level of atherogenic proinflammatory cytokine IFN-γ and the increased level of antiinflammatory cytokine IL-10. Administration of anti-CD25 antibody that depletes Tregs abrogated these atheroprotective effects of G-CSF. The protective effects of G-CSF on atherosclerosis were not recognized in $ApoE^{-/-}/CD28^{-/-}$ double knockout mice. These results suggest that Tregs may play a critical role in the inhibition of atherosclerosis by G-CSF.

The effects of G-CSF on atherosclerosis have been controversial in animal experiments and clinical trials. Previously, we demonstrated that the treatment with G-CSF ameliorates the progression of atherosclerosis using two kinds of rabbit models of atherosclerosis

Please cite this article as: Uchiyama R, et al, Role of regulatory T cells in the atheroprotective effects of granulocyte colony-stimulating factor, J Mol Cell Cardiol (2012), doi:10.1016/j.yjmcc.2011.12.016

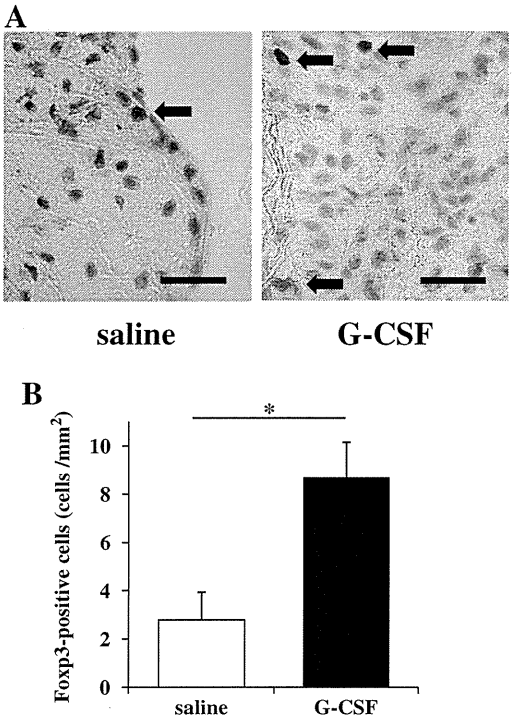

Fig. 5. Effects of G-CSF on Tregs accumulation in atherosclerotic lesion at the aortic sinus. (A) Representative photographs of immunostaining with Foxp3 in the atherosclerotic lesion of the saline-treated mice and the G-CSF-treated mice. Arrows indicate Foxp3-positive cells. (B) The number of Foxp3-positive Tregs in atherosclerosis lesion of the saline-treated and the G-CSF-treated mice. *$P<0.05$. Scale bars indicates 100 μm. The means ± SEM of 10 animals are shown.

[13]. Yoshioka et al. [15] reported that G-CSF treatment accelerated reendothelialization and decreased neointimal formation in mice wire injury model. In contrast, Haghighat et al. [26] showed that G-CSF treatment resulted in the exacerbation of atherosclerosis in ApoE$^{-/-}$ mice. They administered G-CSF subcutaneously to mice at a dose of 10 μg/kg once a day for 5 days per a week on alternating weeks for a total of 20 doses over an 8-week treatment period. The rapid increase and decrease in the number of white blood cell by repeated start and cessation of G-CSF administration may affect the adverse effect on atherosclerosis. Although they showed that G-CSF increases in vessels at adventitia, there is no solid evidence whether the increased vessels at adventitia exacerbate atherosclerosis. Kang et al. [27] reported that G-CSF treatment (10 μg/kg once a day for 4 days before percutaneous coronary intervention (PCI)) increased the risk of in-stent stenosis in patients with acute or old MI. However, number of enrolled patients was small and only a few patients were assessed by coronary angiography at six-month follow-up in the study. Additionally, patients did not receive primary PCI during the golden time of acute MI treatment and PCI was performed under the condition of increasing number of leukocytes by G-CSF. In our clinical trial, G-CSF treatment (2.5 μg/kg once a day for 5 days after PCI) did not affect the restenosis rate in patients with acute MI [12]. Moreover, other randomized clinical trials also reported that G-CSF did not increase the restenosis rate after PCI [28].

The pathogenesis of atherosclerosis is associated with chronic inflammatory mechanisms. The atherosclerotic plaque is characterized by an accumulation of lipids in the artery wall, together with infiltration of immunocytes, such as macrophages, T cells, and mast cells. An increasing body of evidence suggests that the immune system is involved in the process of atherosclerosis [29,30]. T cells are recruited in parallel with macrophages in atherosclerotic lesions and produce proatherogenic mediators. IFN-γ, the signature Th1 cytokine, is present in the human plaque and has pathogenic effects on atherosclerosis [31]. IL-4, the signature Th2 cytokine, is not frequently observed in human plaques, and experimental studies examining the involvement of Th2 cells are contradictory [32]. Several studies have demonstrated a protective effect of Tregs in models of atherosclerosis. CD4$^+$CD25$^+$ Tregs are specialized for the suppression of both Th1 and Th2 pathogenic immune responses against self or foreign antigens and control T cell homeostasis. There has been accumulated evidence indicating that Tregs exert important regulatory functions in various immuno-inflammatory diseases [33]. Tregs play an important role in preventing the spontaneous development of systemic autoimmunity through IL-10 and TGF-β. Zouggari et al. [34] reported that Tregs deletion significantly enhanced postischemic neovascularization by increasing the levels of proinflammatory cytokines. Shi et al. [35] reported that adoptive transfer of Tregs ameliorated coxsackievirus B3-induced myocarditis through suppression of the immune response to heart. TGF-β and phosphorylated Akt levels were upregulated and coxsackie-adenovirus receptor expression was decreased in the heart of the Tregs-transferred mice compared with those in the control mice. Tregs inhibit the functions of activated helper T cells through cell-to-cell contact and soluble inhibitory cytokines such as IL-10 and TGF-β [36]. TGF-β and IL-10 produced by Tregs are reported to have profound atheroprotective effects in mouse models.

G-CSF is a hematopoietic cytokine that stimulates the proliferation and differentiation of normal hematopoietic stem cells. G-CSF mediates immune regulation by inducing apoptosis of T cells and inhibiting proliferation of T cells in response to mitogens [37]. G-CSF stimulation alters the T cell function and modulates the balance between Th1 and Th2 immune responses by affecting cytokine production [17,38]. G-CSF suppresses the productions of proinflammatory cytokines stimulated by lipopolysaccharide in whole blood cells and monocytes [39,40]. In addition to these immune effects, G-CSF mobilizes bone marrow CD4$^+$CD25$^+$ Tregs via reducing the expression of stromal-derived factor in the bone marrow and changing CD4$^+$CD25$^+$ Tregs trafficking [41]. Therefore, we examined whether Tregs are involved in the atheroprotective mechanism of G-CSF. In the present study, G-CSF increased the number of Tregs in spleen and peripheral lymph nodes, and atherosclerotic lesion. Moreover, G-CSF increased the level of IL-10 and decreased the level of IFN-γ in atherosclerotic lesion. IL-10 is reported to inhibit the production of proinflammatory cytokines such as IFN-γ in T cells [36]. These results suggest that G-CSF prevents the progression of atherosclerosis by recruiting Tregs and increasing IL-10 level in plaque. To address the question whether Tregs were implicated in the mechanism of G-CSF-mediated atheroprotective effect, we used two types of Tregs-depleted ApoE$^{-/-}$ mice, which are ApoE$^{-/-}$ mice injected with Treg-depleting antibody (PC61) and ApoE$^{-/-}$/CD28$^{-/-}$ mice. Costimulatory molecule CD28 is required for the generation and homeostasis of Tregs and the number of Tregs is reduced in CD28-deficient mice [22]. Noteworthy, G-CSF treatment exerted no atheroprotective effects in both types of Tregs-depleted ApoE$^{-/-}$ mice. G-CSF-induced decrease in IFN-γ and increase in IL-10 in atherosclerotic plaque were abrogated in Tregs-depleted ApoE$^{-/-}$ mice. These findings suggest that Tregs play an important role in the atheroprotective effects of G-CSF. Some studies reported that TGF-β is a critical mediator of Tregs and others showed that IL-10 is a key molecule of Tregs [3,42,43]. In the present study, TGF-β mRNA in atherosclerotic plaque was not increased by G-CSF, however, we could not exclude the possibility that TGF-β is involved in the G-CSF-induced atheroprotective effect. As some agents including statins and angiotensin-converting enzyme inhibitors are reported to expand Tregs *in vivo* [44,45] modulation of Tregs may become a promising therapeutic target to prevent cardiovascular diseases.

In conclusion, our results demonstrate that G-CSF prevents the progression of atherosclerosis and the increased Tregs are involved in the atheroprotective mechanism of G-CSF in ApoE$^{-/-}$ mice. Further studies including clinical trials are needed to clarify the feasibility and safety of G-CSF-induced atheroprotective effect. In the future, manipulating Tregs by G-CSF or biological agents may provide novel therapeutic strategies for atherosclerosis.

Please cite this article as: Uchiyama R, et al, Role of regulatory T cells in atheroprotective effects of granulocyte colony-stimulating factor, J Mol Cell Cardiol (2012), doi:10.1016/j.yjmcc.2011.12.016

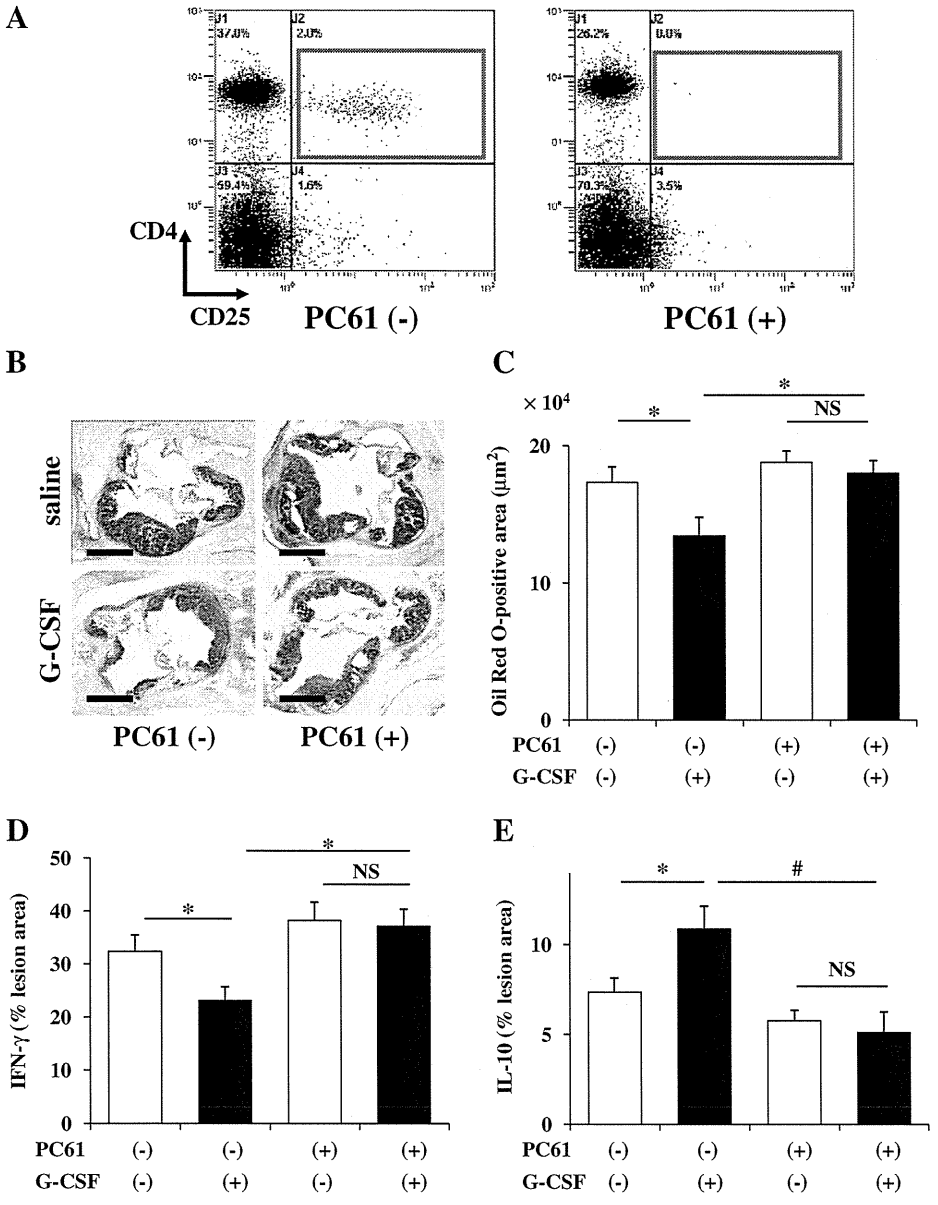

Fig. 6. Atheroprotective effects of G-CSF were abrogated in Tregs-depleted ApoE$^{-/-}$ mice. (A) The proportions of CD4^{+}CD25^{+} Tregs in inguinal lymph nodes from the PC61 or the PBS-treated mice assessed by flow cytometric analysis. (B) Representative photographs of the atherosclerotic lesion formation at the aortic sinus of the saline-treated ApoE$^{-/-}$ mice, the G-CSF-treated ApoE$^{-/-}$ mice, the saline and PC61-treated ApoE$^{-/-}$ mice and the G-CSF and PC61-treated ApoE$^{-/-}$ mice. Sections were taken at the same level of aortic sinus and stained with Oil Red-O as described in Materials and methods. (C) Quantitative analysis of atherosclerotic lesion formation at the aortic sinus in each group. The average lesion area of five sections at the aortic sinus from each mouse was quantified morphometrically after 4 weeks of saline or G-CSF treatment as described in Materials and methods. (D) Quantitative analysis of the level of IFN-γ in atherosclerotic plaque of the Tregs-depleted ApoE$^{-/-}$ mice. (E) Quantitative analysis of the level of IL-10 in atherosclerotic plaque of the Tregs-depleted ApoE$^{-/-}$ mice. $^{*}P<0.05$. $^{\#}P<0.01$. NS indicates that there is no significant difference between the two groups. Scale bars indicates 400 μm. The means ± SEM of 10 animals are shown.

Disclosures

The authors confirm that there are no conflicts of interest.

Acknowledgments

This work was supported by grants from the Ministry of Health Labour and Welfare in Japan and SENSHIN Medical Research Foundation. The authors thank Ryo Abe (Research Institute for Biological Sciences, Science University of Tokyo, Chiba, Japan) for kindly gift of CD28$^{-/-}$ mice. The authors also thank Akane Furuyama, Yuko Ohtsuki, Megumi Ikeda, Ikuko Sakamoto, Megumi Iiyama and Miho Kikuchi for their excellent technical assistance.

References

[1] Galkina E, Ley K. Immune and inflammatory mechanisms of atherosclerosis. Annu Rev Immunol 2009;27:165–97.
[2] Huehn J, Polansky JK, Hamann A. Epigenetic control of FOXP3 expression: the key to a stable regulatory T-cell lineage? Nat Rev Immunol 2009;9:83–9.
[3] Ait-Oufella H, Salomon BL, Potteaux S, Robertson AK, Gourdy P, Zoll J, et al. Natural regulatory T cells control the development of atherosclerosis in mice. Nat Med 2006;12:178–80.
[4] Mallat Z, Gojova A, Brun V, Esposito B, Fournier N, Cottrez F, et al. Induction of a regulatory T cell type 1 response reduces the development of atherosclerosis in apolipoprotein E-knockout mice. Circulation 2003;108:1232–7.
[5] Sakaguchi S. Naturally arising Foxp3-expressing CD25+CD4+ regulatory T cells in immunological tolerance to self and non-self. Nat Immunol 2005;6:345–52.
[6] Takahashi T, Kalka C, Masuda H, Chen D, Silver M, Kearney M, et al. Ischemia- and cytokine-induced mobilization of bone marrow-derived endothelial progenitor cells for neovascularization. Nat Med 1999;5:434–8.

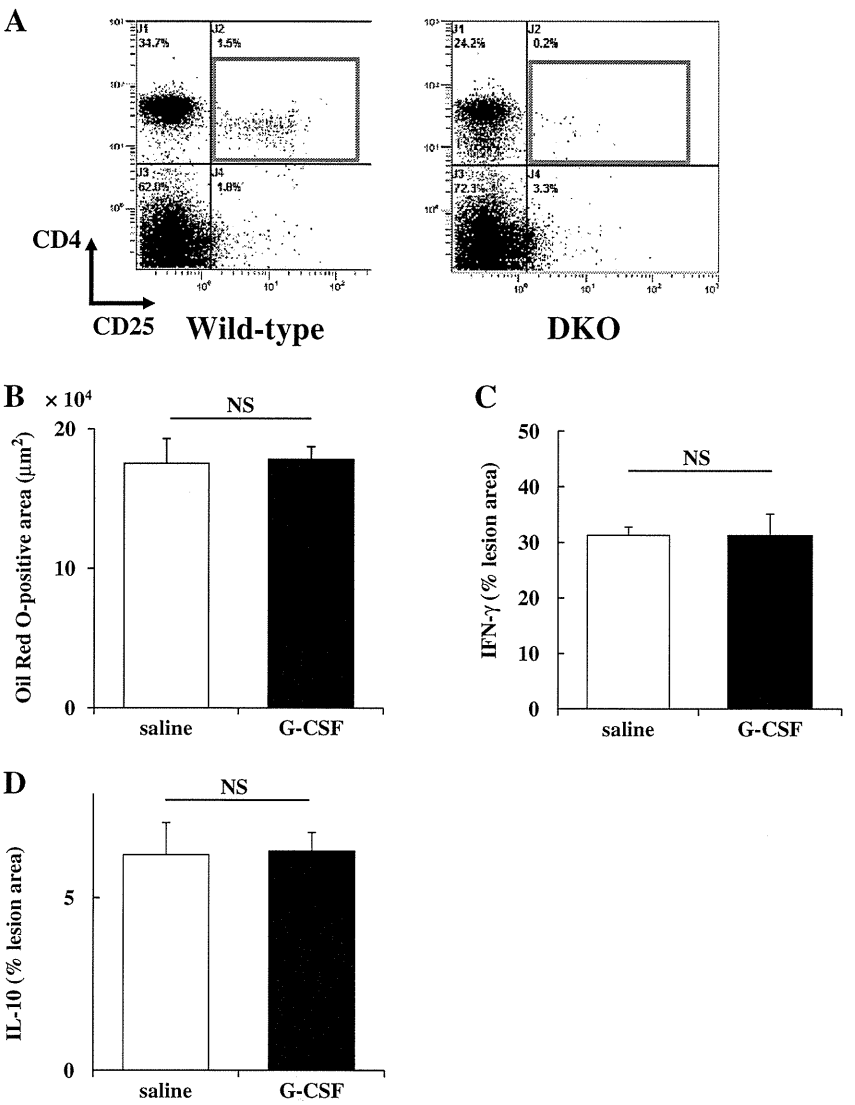

Fig. 7. Atheroprotective effects of G-CSF were abrogated in ApoE$^{-/-}$/CD28$^{-/-}$ mice. (A) The proportions of CD4^{+}CD25^{+} Tregs in inguinal lymph nodes from wild type mice and DKO mice assessed by flow cytometric analysis. (B) Quantitative analysis of atherosclerotic lesion formation at the aortic sinus in ApoE$^{-/-}$/CD28$^{-/-}$ mice. The average lesion area of five sections at the aortic sinus from each mouse was quantified morphometrically after 4 weeks of saline or G-CSF treatment as described in Materials and methods. (C) Quantitative analysis of the level of IFN-γ in atherosclerotic plaque of the DKO mice. (D) Quantitative analysis of the level of IL-10 in atherosclerotic plaque of the DKO mice. NS indicates that there is no significant difference between the two groups. The means ± SEM of 9 animals are shown.

[7] Rutella S, Zavala F, Danese S, Kared H, Leone G. Granulocyte colony-stimulating factor: a novel mediator of T cell tolerance. J Immunol 2005;175:7085–91.
[8] Harada M, Qin Y, Takano H, Minamino T, Zou Y, Toko H, et al. G-CSF prevents cardiac remodeling after myocardial infarction by activating the Jak-Stat pathway in cardiomyocytes. Nat Med 2005;11:305–11.
[9] Ince H, Petzsch M, Kleine HD, Schmidt H, Rehders T, Korber T, et al. Preservation from left ventricular remodeling by front-integrated revascularization and stem cell liberation in evolving acute myocardial infarction by use of granulocyte-colony-stimulating factor (FIRSTLINE-AMI). Circulation 2005;112:3097–106.
[10] Minatoguchi S, Takemura G, Chen XH, Wang N, Uno Y, Koda M, et al. Acceleration of the healing process and myocardial regeneration may be important as a mechanism of improvement of cardiac function and remodeling by postinfarction granulocyte colony-stimulating factor treatment. Circulation 2004;109:2572–80.
[11] Ohtsuka M, Takano H, Zou Y, Toko H, Akazawa H, Qin Y, et al. Cytokine therapy prevents left ventricular remodeling and dysfunction after myocardial infarction through neovascularization. FASEB J 2004;18:851–3.
[12] Takano H, Hasegawa H, Kuwabara Y, Nakayama T, Matsuno K, Miyazaki Y, et al. Feasibility and safety of granulocyte colony-stimulating factor treatment in patients with acute myocardial infarction. Int J Cardiol 2007;122:41–7.
[13] Hasegawa H, Takano H, Ohtsuka M, Ueda K, Niitsuma Y, Qin Y, et al. G-CSF prevents the progression of atherosclerosis and neointimal formation in rabbits. Biochem Biophys Res Commun 2006;344:370–6.
[14] Kong D, Melo LG, Gnecchi M, Zhang L, Mostoslavsky G, Liew CC, et al. Cytokine-induced mobilization of circulating endothelial progenitor cells enhances repair of injured arteries. Circulation 2004;110:2039–46.
[15] Yoshioka T, Takahashi M, Shiba Y, Suzuki C, Morimoto H, Izawa A, et al. Granulocyte colony-stimulating factor (G-CSF) accelerates reendothelialization and reduces neointimal formation after vascular injury in mice. Cardiovasc Res 2006;70:61–9.
[16] Matsumoto T, Watanabe H, Ueno T, Tsunemi A, Hatano B, Kusumi Y, et al. Appropriate doses of granulocyte-colony stimulating factor reduced atherosclerotic plaque formation and increased plaque stability in cholesterol-fed rabbits. J Atheroscler Thromb 2010;17:84–96.
[17] Sloand EM, Kim S, Maciejewski JP, Van Rhee F, Chaudhuri A, Barrett J, et al. Pharmacologic doses of granulocyte colony-stimulating factor affect cytokine production by lymphocytes in vitro and in vivo. Blood 2000;95:2269–74.
[18] Reyes E, Garcia-Castro I, Esquivel F, Hornedo J, Cortes-Funes H, Solovera J, et al. Granulocyte colony-stimulating factor (G-CSF) transiently suppresses mitogen-stimulated T-cell proliferative response. Br J Cancer 1999;80:229–35.
[19] Kared H, Masson A, Adle-Biassette H, Bach JF, Chatenoud L, Zavala F. Treatment with granulocyte colony-stimulating factor prevents diabetes in NOD mice by recruiting plasmacytoid dendritic cells and functional CD4(+)CD25(+) regulatory T-cells. Diabetes 2005;54:78–84.
[20] Liang HL, Yi DH, Zheng QJ, Du JF, Cao YX, Yu SQ, et al. Improvement of heart allograft acceptability associated with recruitment of CD4+CD25 + T cells in peripheral blood by recipient treatment with granulocyte colony-stimulating factor. Transplant Proc 2008;40:1604–11.
[21] Paigen B, Morrow A, Holmes PA, Mitchell D, Williams RA. Quantitative assessment of atherosclerotic lesions in mice. Atherosclerosis 1987;68:231–40.
[22] Shahinian A, Pfeffer K, Lee KP, Kundig TM, Kishihara K, Wakeham A, et al. Differential T cell costimulatory requirements in CD28-deficient mice. Science 1993;261:609–12.

[23] Hu Y, Zhang H, Lu Y, Bai H, Xu Y, Zhu X, et al. Class A scavenger receptor attenuates myocardial infarction-induced cardiomyocyte necrosis through suppressing M1 macrophage subset polarization. Basic Res Cardiol 2011;106:1311–28.
[24] Leucht C, Stigloher C, Wizenmann A, Klafke R, Folchert A, Bally-Cuif L. MicroRNA-9 directs late organizer activity of the midbrain-hindbrain boundary. Nat Neurosci 2008;11:641–8.
[25] Gotsman I, Grabie N, Gupta R, Dacosta R, MacConmara M, Lederer J, et al. Impaired regulatory T-cell response and enhanced atherosclerosis in the absence of inducible costimulatory molecule. Circulation 2006;114:2047–55.
[26] Haghighat A, Weiss D, Whalin MK, Cowan DP, Taylor WR. Granulocyte colony-stimulating factor and granulocyte macrophage colony-stimulating factor exacerbate atherosclerosis in apolipoprotein E-deficient mice. Circulation 2007;115: 2049–54.
[27] Kang HJ, Kim HS, Zhang SY, Park KW, Cho HJ, Koo BK, et al. Effects of intracoronary infusion of peripheral blood stem-cells mobilised with granulocyte-colony stimulating factor on left ventricular systolic function and restenosis after coronary stenting in myocardial infarction: the MAGIC cell randomised clinical trial. Lancet 2004;363:751–6.
[28] Takano H, Ueda K, Hasegawa H, Komuro I. G-CSF therapy for acute myocardial infarction. Trends Pharmacol Sci 2007;28:512–7.
[29] Binder CJ, Chang MK, Shaw PX, Miller YI, Hartvigsen K, Dewan A, et al. Innate and acquired immunity in atherogenesis. Nat Med 2002;8:1218–26.
[30] Hansson GK. Inflammation, atherosclerosis, and coronary artery disease. N Engl J Med 2005;352:1685–95.
[31] Hansson GK, Hermansson A. The immune system in atherosclerosis. Nat Immunol 2011;12:204–12.
[32] Davenport P, Tipping PG. The role of interleukin-4 and interleukin-12 in the progression of atherosclerosis in apolipoprotein E-deficient mice. Am J Pathol 2003;163: 1117–25.
[33] Sakaguchi S, Fukuma K, Kuribayashi K, Masuda T. Organ-specific autoimmune diseases induced in mice by elimination of T cell subset. I. Evidence for the active participation of T cells in natural self-tolerance; deficit of a T cell subset as a possible cause of autoimmune disease. J Exp Med 1985;161:72–87.
[34] Zouggari Y, Ait-Oufella H, Waeckel L, Vilar J, Loinard C, Cochain C, et al. Regulatory T cells modulate postischemic neovascularization. Circulation 2009;120: 1415–25.
[35] Shi Y, Fukuoka M, Li G, Liu Y, Chen M, Konviser M, et al. Regulatory T cells protect mice against coxsackievirus-induced myocarditis through the transforming growth factor beta-coxsackie-adenovirus receptor pathway. Circulation 2010;121:2624–34.
[36] Taleb S, Tedgui A, Mallat Z. Regulatory T-cell immunity and its relevance to atherosclerosis. J Intern Med 2008;263:489–99.
[37] Rutella S, Rumi C, Testa U, Sica S, Teofili L, Martucci R, et al. Inhibition of lymphocyte blastogenic response in healthy donors treated with recombinant human granulocyte colony-stimulating factor (rhG-CSF): possible role of lactoferrin and interleukin-1 receptor antagonist. Bone Marrow Transplant 1997;20:355–64.
[38] Pan L, Delmonte Jr J, Jalonen CK, Ferrara JL. Pretreatment of donor mice with granulocyte colony-stimulating factor polarizes donor T lymphocytes toward type-2 cytokine production and reduces severity of experimental graft-versus-host disease. Blood 1995;86:4422–9.
[39] Boneberg EM, Hareng L, Gantner F, Wendel A, Hartung T. Human monocytes express functional receptors for granulocyte colony-stimulating factor that mediate suppression of monokines and interferon-gamma. Blood 2000;95:270–6.
[40] Boneberg EM, Hartung T. Granulocyte colony-stimulating factor attenuates LPS-stimulated IL-1beta release via suppressed processing of proIL-1beta, whereas TNF-alpha release is inhibited on the level of proTNF-alpha formation. Eur J Immunol 2002;32:1717–25.
[41] Zou L, Barnett B, Safah H, Larussa VF, Evdemon-Hogan M, Mottram P, et al. Bone marrow is a reservoir for CD4+CD25+ regulatory T cells that traffic through CXCL12/CXCR4 signals. Cancer Res 2004;64:8451–5.
[42] Kinsey GR, Sharma R, Huang L, Li L, Vergis AL, Ye H, et al. Regulatory T cells suppress innate immunity in kidney ischemia-reperfusion injury. J Am Soc Nephrol 2009;20: 1744–53.
[43] Liesz A, Suri-Payer E, Veltkamp C, Doerr H, Sommer C, Rivest S, et al. Regulatory T cells are key cerebroprotective immunomodulators in acute experimental stroke. Nat Med 2009;15:192–9.
[44] Mira E, Leon B, Barber DF, Jimenez-Baranda S, Goya I, Almonacid L, et al. Statins induce regulatory T cell recruitment via a CCL1 dependent pathway. J Immunol 2008;181: 3524–34.
[45] Platten M, Youssef S, Hur EM, Ho PP, Han MH, Lanz TV, et al. Blocking angiotensin-converting enzyme induces potent regulatory T cells and modulates TH1- and TH17-mediated autoimmunity. Proc Natl Acad Sci U S A 2009;106:14948–53.

Please cite this article as: Uchiyama R, et al, Role of regulatory T cells in the atheroprotective effects of granulocyte colony-stimulating factor, J Mol Cell Cardiol (2012), doi:10.1016/j.yjmcc.2011.12.016

Cell Metabolism
Article

p53-Induced Adipose Tissue Inflammation Is Critically Involved in the Development of Insulin Resistance in Heart Failure

Ippei Shimizu,[1,5] Yohko Yoshida,[1,5] Taro Katsuno,[1] Kaoru Tateno,[1] Sho Okada,[1] Junji Moriya,[1] Masataka Yokoyama,[1] Aika Nojima,[1] Takashi Ito,[1] Rudolf Zechner,[2] Issei Komuro,[3] Yoshio Kobayashi,[1] and Tohru Minamino[1,4,*]
[1]Department of Cardiovascular Science and Medicine, Chiba University Graduate School of Medicine, Chiba 260-8670, Japan
[2]Institute of Molecular Biosciences, University of Graz, A-8010 Graz, Austria
[3]Department of Cardiovascular Medicine, Osaka University School of Medicine, Osaka 565-0871, Japan
[4]PRESTO, Japan Science and Technology Agency, Saitama 332-0012, Japan
[5]These authors contributed equally to this work
*Correspondence: t_minamino@yahoo.co.jp
DOI 10.1016/j.cmet.2011.12.006

SUMMARY

Several clinical studies have shown that insulin resistance is prevalent among patients with heart failure, but the underlying mechanisms have not been fully elucidated. Here, we report a mechanism of insulin resistance associated with heart failure that involves upregulation of p53 in adipose tissue. We found that pressure overload markedly upregulated p53 expression in adipose tissue along with an increase of adipose tissue inflammation. Chronic pressure overload accelerated lipolysis in adipose tissue. In the presence of pressure overload, inhibition of lipolysis by sympathetic denervation significantly downregulated adipose p53 expression and inflammation, thereby improving insulin resistance. Likewise, disruption of p53 activation in adipose tissue attenuated inflammation and improved insulin resistance but also ameliorated cardiac dysfunction induced by chronic pressure overload. These results indicate that chronic pressure overload upregulates adipose tissue p53 by promoting lipolysis via the sympathetic nervous system, leading to an inflammatory response of adipose tissue and insulin resistance.

INTRODUCTION

The p53 tumor suppressor pathway coordinates DNA repair, cell-cycle arrest, apoptosis, and senescence to preserve genomic stability and prevent oncogenesis. Activation of p53 is driven by a wide variety of stress signals that have the potential to promote tumor formation, such as DNA damage, telomere shortening, oxidative stress, and oncogene activation (Harris and Levine, 2005; Meek, 2009; Vousden and Prives, 2009). Recently, the contribution of p53 to many undesirable aspects of aging and age-associated diseases, such as cardiovascular and metabolic disorders, has been recognized (Royds and Iacopetta, 2006; Vousden and Lane, 2007). It has been reported that aging is associated with an increase of the p53-mediated transcriptional activity (Edwards et al., 2007) and that slight constitutive overactivation of p53 is associated with premature aging in mice (Maier et al., 2004; Tyner et al., 2002). Activation of p53 has also been observed in aged vessels and failing hearts and has been implicated in atherosclerosis and heart failure (Minamino and Komuro, 2007, 2008; Sano et al., 2007). Recent findings have indicated a role of p53 in determining the response of cells to nutrient stress and in regulating metabolism (Vousden and Ryan, 2009). It has also been demonstrated that excessive calorie intake induces p53-induced inflammation in adipose tissue, leading to insulin resistance and diabetes in mice (Minamino et al., 2009).

A close link between heart failure and diabetes has long been recognized in the clinical setting (Ashrafian et al., 2007; Lopaschuk et al., 2007; Witteles and Fowler, 2008). Many mechanisms have been suggested to explain the increased incidence of heart failure in diabetic patients, including the hypertrophic influence of insulin, the adverse effects of hyperglycemia, increased oxidative stress, and hyperactivity of neurohumoral systems, such as the renin-angiotensin-aldosterone system and the adrenergic system. Recently, increasing attention has been paid to insulin resistance as a distinct cause of cardiac dysfunction and heart failure in diabetic patients. A study of Swedish patients without prior cardiac dysfunction found that insulin resistance predicted the subsequent onset of heart failure independently of established risk factors (Ingelsson et al., 2005). In another clinical study, the plasma level of proinsulin (a marker of insulin resistance) was found to be higher in patients who subsequently developed heart failure than in control patients 20 years before the actual diagnosis of heart failure (Arnlöv et al., 2001). These findings indicate that insulin resistance precedes heart failure rather than being a consequence of it. Evidence has emerged that myocardial insulin resistance is central to altered metabolism in the failing heart and may play a crucial role in the development of heart failure (Ashrafian et al., 2007; Lopaschuk et al., 2007; Witteles and Fowler, 2008). The adaptive response of the failing heart involves a complex series of enzymatic shifts and changes in the regulation of transcriptional factors, which result in an increase of glucose metabolism and a decrease of fatty acid metabolism

to maximize the efficacy of energy production (Neubauer, 2007). Insulin resistance of the myocardium inhibits these adaptive responses, leading to increased reliance on fatty acid metabolism. This increases oxygen consumption and decreases cardiac function, raising the potential for lipotoxicity in the heart (Sharma et al., 2007; Young et al., 2002). Another line of evidence indicates that insulin signaling is upregulated in the failing heart and that excessive cardiac insulin signaling exacerbates systolic dysfunction (Shimizu et al., 2010).

Moreover, there is increasing evidence that heart failure reciprocally augments the risk of insulin resistance and clinical diabetes (Ashrafian et al., 2007). Insulin resistance and abnormal glucose metabolism are very common in heart failure patients, being identified in 43% of these patients, and such abnormalities are associated with decreased cardiac function (Suskin et al., 2000). Surprisingly, the link between heart failure and insulin resistance grows stronger when patients with ischemic heart disease are excluded (Witteles and Fowler, 2008). Heart failure also predicts the development of type 2 diabetes in a graded way (Tenenbaum et al., 2003). Although the above mentioned clinical evidence supports a role of insulin resistance in the occurrence of heart failure, evidence for the reciprocal statement that heart failure promotes insulin resistance is largely associative. Moreover, the role of heart failure in the promotion of insulin resistance has been demonstrated by only a few animal studies (Nikolaidis et al., 2004; Shimizu et al., 2010) and the underlying mechanisms are largely speculative.

Here, we studied the role of heart failure in the development of insulin resistance and sought to elucidate the molecular mechanisms involved. We found that insulin resistance developed in two murine models of heart failure, a chronic pressure overload model and a myocardial infarction model. Heart failure markedly upregulated p53 expression in adipose tissue in association with increased inflammation of adipose tissue. Heart failure accelerated lipolysis in adipose tissue, whereas inhibition of lipolysis by sympathetic denervation or treatment with a lipase inhibitor significantly downregulated adipose tissue p53 expression and inflammation, thereby improving insulin resistance. Likewise, disruption of p53 activation in adipose tissue not only ameliorated inflammation in this tissue and improved insulin resistance but also improved cardiac dysfunction associated with heart failure. We conclude that heart failure upregulates p53 in adipose tissue by promoting lipolysis via activation of the sympathetic nervous system, leading to an inflammatory response of adipose tissue and insulin resistance. Our results indicate that inhibition of p53-induced adipose inflammation is a potential target for treating metabolic abnormalities and systolic dysfunction in patients with heart failure.

RESULTS

Pressure Overload Induces Adipose Tissue Inflammation and Insulin Resistance

To examine the effect of cardiac pressure overload on glucose homeostasis, we produced transverse aortic constriction (TAC) in 11-week-old mice. In this mouse model, systolic cardiac function deteriorated significantly along with left ventricular (LV) dilatation 2–6 weeks after surgery (Figure S1A available online). The insulin tolerance test (ITT) and the glucose tolerance test (GTT) showed that insulin sensitivity and glucose tolerance were impaired at 4–6 weeks after TAC (Figure 1A) without any change of food intake (Figure S1B). In patients with metabolic disorders, the recruitment of inflammatory macrophages to adipose tissue has been shown to increase the production of proinflammatory cytokines, such as tumor necrosis factor (TNF)-α and chemokine (C–C motif) ligand 2 (CCL2), also known as monocyte chemoattractant protein-1 (MCP-1), leading to the development of systemic insulin resistance (Hotamisligil et al., 1993; Kamei et al., 2006; Weisberg et al., 2003). Therefore, we investigated whether pressure overload provokes adipose tissue inflammation. Examination of hematoxylin- and eosin-stained sections demonstrated the infiltration of mononuclear cells into visceral fat, with most of these cells being identified as macrophages by immunofluorescent staining for Mac3 (Figure 1B). Consistent with these results, expression of a marker for macrophages (Egf-like module containing, mucin-like, hormone receptor-like 1; EMR1) and production of proinflammatory cytokines were significantly upregulated in the adipose tissue of TAC mice along with a decrease of adiponectin (Figure 1C) compared with sham-operated mice. Treatment of TAC mice with a neutralizing antibody for Tnf-α significantly improved insulin resistance and glucose intolerance, suggesting a crucial role in the upregulation of proinflammatory cytokines in the development of metabolic abnormalities during heart failure (Figure S1C).

Pressure Overload Increases Lipolysis and Induces p53-Dependent Inflammation in Adipose Tissue during Heart Failure

Computed tomography (CT) showed a significant decrease of visceral fat after the creation of pressure overload (Figure 1D). It is well accepted that sympathetic activity increases with heart failure (Floras, 2009), and norepinephrine regulates lipolysis in adipose tissue. We found that the norepinephrine levels of plasma and adipose tissue increased significantly and plasma fatty acid levels were markedly elevated in TAC mice compared with sham-operated mice, suggesting acceleration of lipolysis via the sympathetic nervous system in response to pressure overload (Figure 1E). It has been reported that exposure to an excess of fatty acids leads to p53 activation in various cells (Zeng et al., 2008) and that p53 is crucially involved in the regulation of adipose tissue inflammation in obese animals (Minamino et al., 2009). Therefore, we hypothesized that chronic pressure overload promotes lipolysis and the resultant increase of fatty acids leads to p53-induced inflammation in adipose tissue.

Consistent with this concept, we found that p53 expression was upregulated in the adipose tissue of TAC mice at 2–4 weeks after surgery and the change was sustained until 6 weeks (Figures 2A and S2A). To further investigate the role of adipose tissue p53 in the response to pressure overload, we performed TAC in adipocyte-specific p53 knockout (adipo-p53 KO) mice. The pressure overload-induced increase of p53 expression was attenuated in adipo-p53 KO mice compared with littermate controls (Figure S2B). Production of proinflammatory cytokines as well as cyclin-dependent kinase inhibitor 1A (*Cdkn1a*) expression was also decreased in adipo-p53 KO mice, along with a decline in the infiltration of macrophages into visceral fat

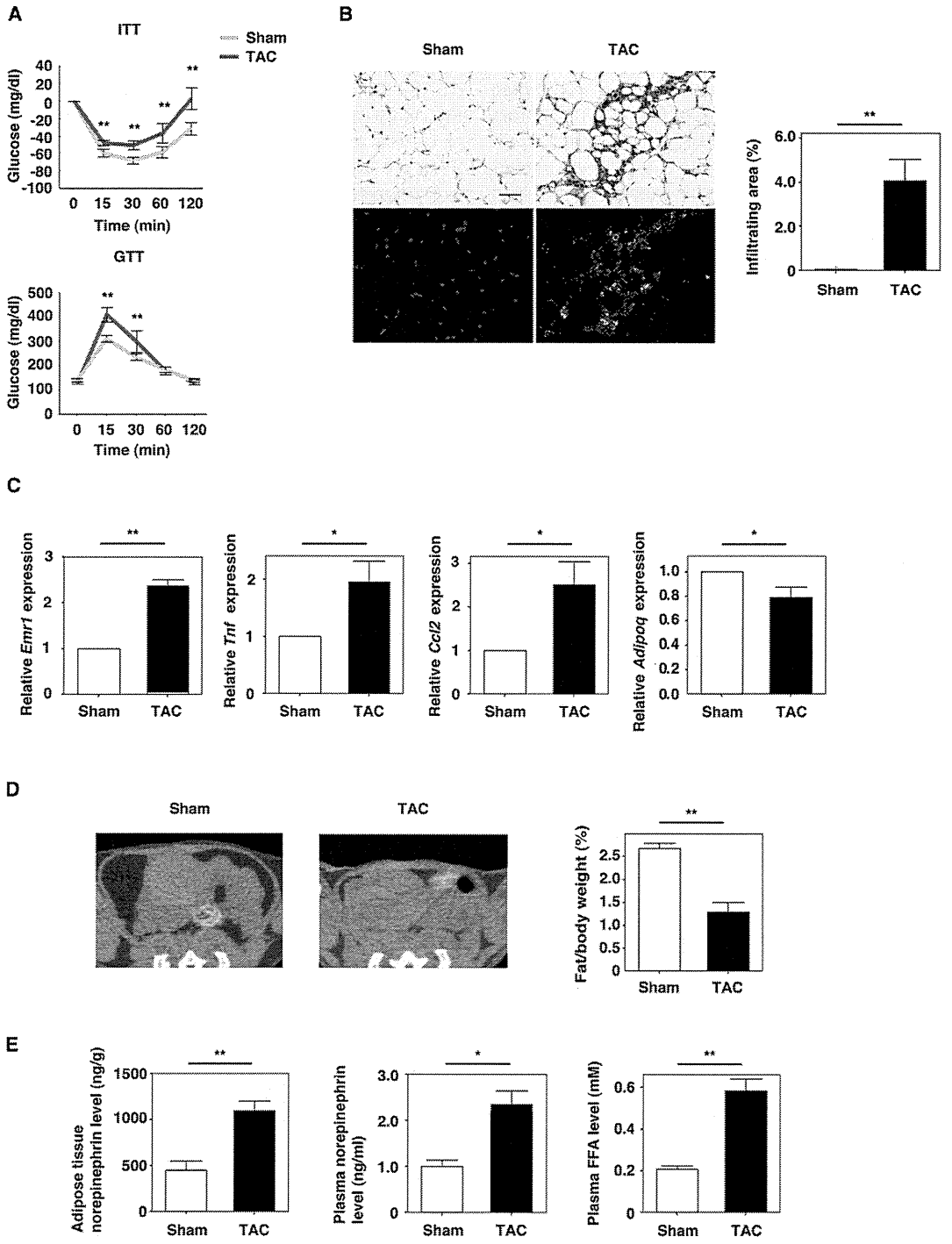

Figure 1. Pressure Overload Induces Systemic Insulin Resistance and Adipose Tissue Lipolysis and Inflammation

(A) Insulin tolerance test (ITT) and glucose tolerance test (GTT) in mice at 6 weeks after sham operation (Sham) or TAC (n = 30).

(B) Hematoxylin and eosin staining of adipose tissues of mice at 6 weeks after sham operation (Sham) or TAC (upper panel). In the lower panel, the infiltration of macrophages was evaluated by immunofluorescent staining for Mac3 (green). Nuclei were stained with Hoechst dye (blue). Scale bar, 50 μm. The right graph indicates the quantitative data on the infiltration of macrophages (n = 5).

(C) Real-time PCR assessing the expression of *Emr1*, *Tnf* (Tnfα), *Ccl2* (MCP1), and *Adipoq* (Adiponectin) levels in adipose tissues of mice at 6 weeks after sham operation (Sham) or TAC (n = 10).

(D) CT analysis of mice at 6 weeks after sham operation (Sham) or TAC. The graph shows the ratio of visceral fat tissue weight estimated by CT to whole body weight (n = 7).

(E) Norepinephrine level in adipose tissue (left) and plasma (middle), and plasma free fatty acid (FFA) level (right) of mice at 6 weeks after sham operation (Sham) or TAC (n = 10). Data are shown as the means ± S.E.M. *p < 0.05, **p < 0.01.

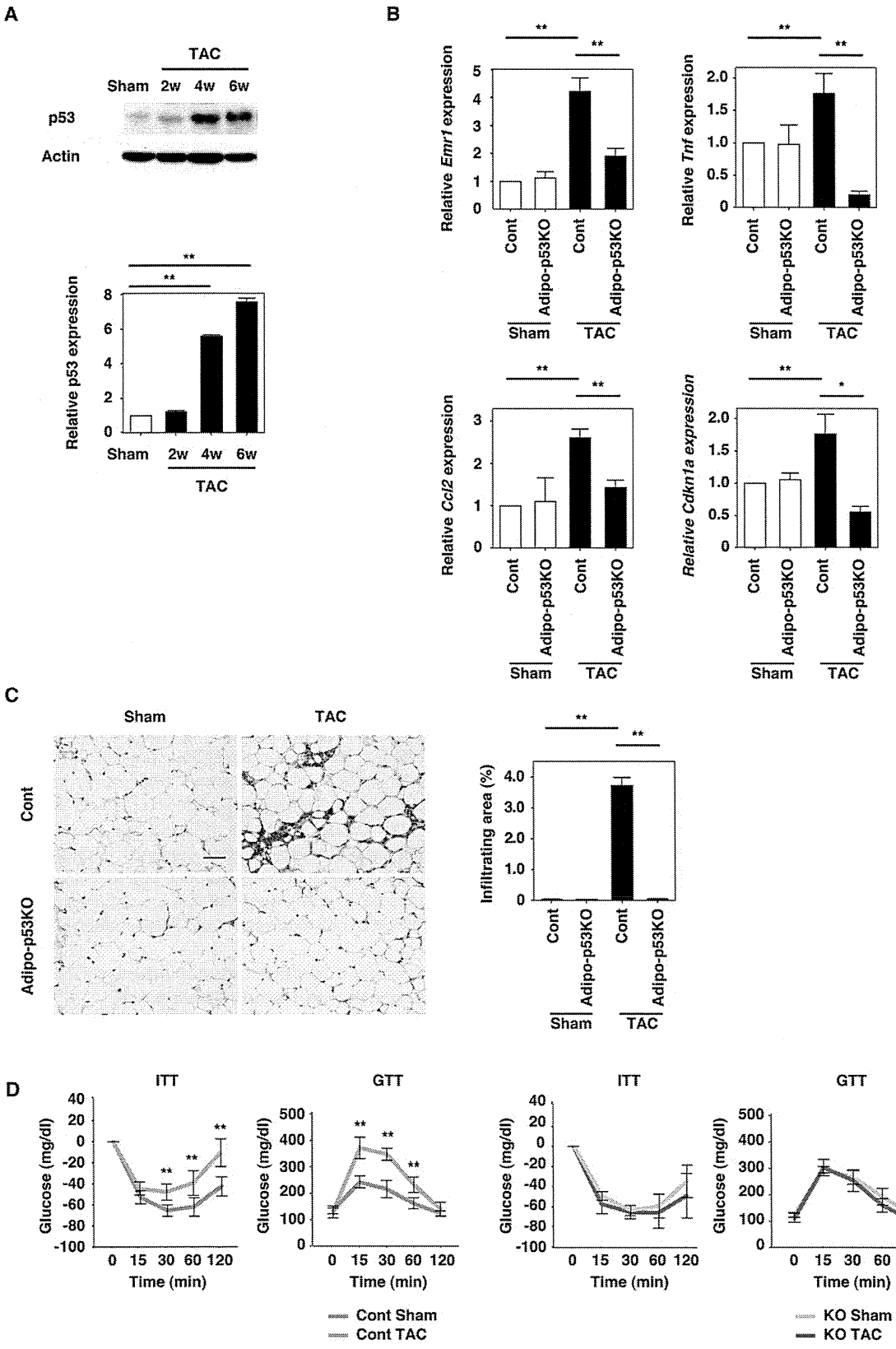
A
TAC
Sham 2w 4w 6w
p53
Actin
Relative p53 expression
Sham 2w 4w 6w
TAC
B
Relative Emr1 expression
Relative Tnf expression
Relative Ccl2 expression
Relative Cdkn1a expression
Cont
Adipo-p53KO
Sham
TAC
C
Sham
TAC
Cont
Adipo-p53KO
Infiltrating area (%)
D
ITT
GTT
Glucose (mg/dl)
Time (min)
Cont Sham
Cont TAC
KO Sham
KO TAC

(Figures 2B and 2C). Consequently, adipo-p53 KO mice showed improved insulin sensitivity and glucose tolerance after induction of pressure overload compared with littermate controls (Figure 2D) without any change of food intake (Figure S2C). These results suggest that p53 has a critical role in the regulation of adipose tissue inflammation and insulin resistance during pressure overload. In contrast, a decrease of fat mass and an increase of plasma free fatty acids were observed to a similar extent in both adipo-p53 KO and control mice after TAC (Figures S2D–S2F), suggesting that pressure overload accelerates lipolysis in a p53-independent manner.

Pressure Overload Promotes Lipolysis via the Sympathetic Nervous System

We inhibited sympathetic activity in epididymal fat tissue by surgical denervation and then performed TAC. As a result, surgical denervation effectively inhibited an increase of the norepinephrine level of adipose tissue and attenuated lipolysis after the onset of pressure overload (Figures S3A and S3B and data not shown). Histological examination of adipose tissue showed that infiltration of inflammatory cells after TAC was attenuated by denervation (Figures S3C and S3D). Likewise, disruption of the sympathetic efferent nerves significantly reduced pressure overload-induced upregulation of *Emr1*, a proinflammatory cytokine expression in adipose tissue (Figure 3A), and this reduction was associated with significant improvement of insulin resistance and glucose tolerance in TAC mice (Figure 3B). Surgical denervation attenuated pressure overload-induced upregulation of p53 and *Cdkn1a* expression in adipose tissue (Figures 3A and 3C). We also pharmacologically inhibited the sympathetic activity in adipose tissue by injecting guanethidine directly into epididymal fat and then performed TAC. As a result, pharmacological denervation also significantly inhibited lipolysis (Figures S3A and S3B) and attenuated upregulation of p53 and *Cdkn1a* expression and inflammation in adipose tissues (Figures S3C, S3D, S4A and S4B). Mice treated with guanethidine showed better insulin sensitivity and glucose tolerance after creation of pressure overload (Figure S4C), indicating that pressure overload-induced activation of the sympathetic nervous system accelerates lipolysis and, thus, leads to adipose tissue inflammation and insulin resistance in TAC mice.

Role of Lipolysis in the Regulation of Adipose p53 Expression and Inflammation

To examine the role of lipolysis in influencing adipose tissue expression of p53 and inflammation after TAC, we inhibited lipolysis by administering acipimox, a selective inhibitor of lipolysis, to mice with TAC. Treatment with acipimox markedly inhibited lipolysis and also reduced infiltration of inflammatory cells into adipose tissue during pressure overload (Figures S3A–S3D). Inhibition of lipolysis also significantly reduced pressure overload-induced upregulation of *Emr1* and proinflammatory cytokine production in adipose tissue (Figure 4A), along with significant improvement of insulin resistance and glucose intolerance in TAC mice (Figure 4B). Furthermore, treatment with acipimox attenuated pressure overload-induced upregulation of p53 and *Cdkn1a* expression in adipose tissue (Figures 4A and 4C), confirming a close relationship between lipolysis and p53 expression.

Next, we promoted lipolysis by administering isoproterenol to mice via an infusion pump. Treatment with isoproterenol significantly decreased the visceral fat mass and increased plasma fatty acid levels (Figures S5A–S5C) and increased p53 expression in adipose tissue (Figure 5A). Isoproterenol also induced adipose tissue inflammation (Figures 5B and 5C). To further investigate the role of lipolysis in the regulation of p53 expression and inflammation in adipose tissue, we tested the influence of deleting adipose triglyceride lipase (patatin-like phospholipase domain containing protein 2, encoded by *Pnpla2*; hereafter referred to as Atgl) on adipose tissue expression of p53. It has been reported that Atgl homozygous KO mice show massive accumulation of lipids in the heart, causing cardiac dysfunction and premature death (Haemmerle et al., 2006). When we generated TAC mice, we also noted that cardiac function was worse and LV enlargement was more marked in Atgl heterozygous KO mice compared with their littermates (Figure S5D). In fact, most of the KO mice died of heart failure within 4 weeks after TAC. Therefore, we utilized Atgl-deficient adipose tissue for ex vivo experiments. We cultured epididymal fat pad tissues from Atgl KO mice or wild-type littermates and examined the effect of isoproterenol on p53 expression. Treatment of wild-type fat pads with isoproterenol significantly induced lipolysis (Figure 5D) and upregulated the expression of both p53 and *Cdkn1a* expression (Figures 5E and 5F). Disruption of Atgl inhibited isoproterenol-induced lipolysis (Figure 5D) and prevented the upregulation of adipose p53 and *Cdkn1a* expression (Figures 5E and 5F), suggesting a crucial role of lipolysis in the regulation of p53 expression and inflammation in adipose tissue.

Myocardial Infarction Induces Adipose Tissue Inflammation and Insulin Resistance

To investigate whether myocardial infarction (MI) induced insulin resistance, we created MI in 11-week-old mice and assessed the animals 6 weeks after surgery. Insulin sensitivity and glucose tolerance were significantly impaired in MI mice compared with sham-operated mice (Figure S5E). Significant loss of fat tissue was also observed in MI mice (Figures S5F and S5G) and this was associated with upregulation of adipose

Figure 2. p53-Dependent Adipose Tissue Inflammation Provokes Systemic Insulin Resistance during Heart Failure

(A) Expression of p53 was examined in adipose tissues of mice by western blot analysis at indicated time points after sham operation (Sham) or TAC. Actin was used as an equal loading control. The graph indicates the quantitative data on p53 expression (n = 3).

(B) Real-time PCR assessing the expression of *Emr1*, *Tnf* (Tnfα), *Ccl2* (MCP1), and *Cdkn1a* (p21) levels in adipose tissue of adipocyte-specific p53-deficient mice (adipo-p53 KO) and littermate controls (Cont) at 6 weeks after sham operation or TAC procedure (n = 12).

(C) Hematoxylin and eosin staining of adipose tissues of adipocyte-specific p53-deficient mice (adipo-p53 KO) and littermate controls (Cont) at 6 weeks after sham operation (Sham) or TAC procedure. Scale bar, 50 μm. The right graph indicates the quantitative data on the infiltration of macrophages (n = 4).

(D) Insulin tolerance test (ITT) and glucose tolerance test (GTT) in adipocyte-specific p53-deficient mice (KO) and littermate controls (Cont) at 6 weeks after sham operation (Sham) or TAC procedure (n = 16). Data are shown as the means ± S.E.M. *$p < 0.05$, **$p < 0.01$.

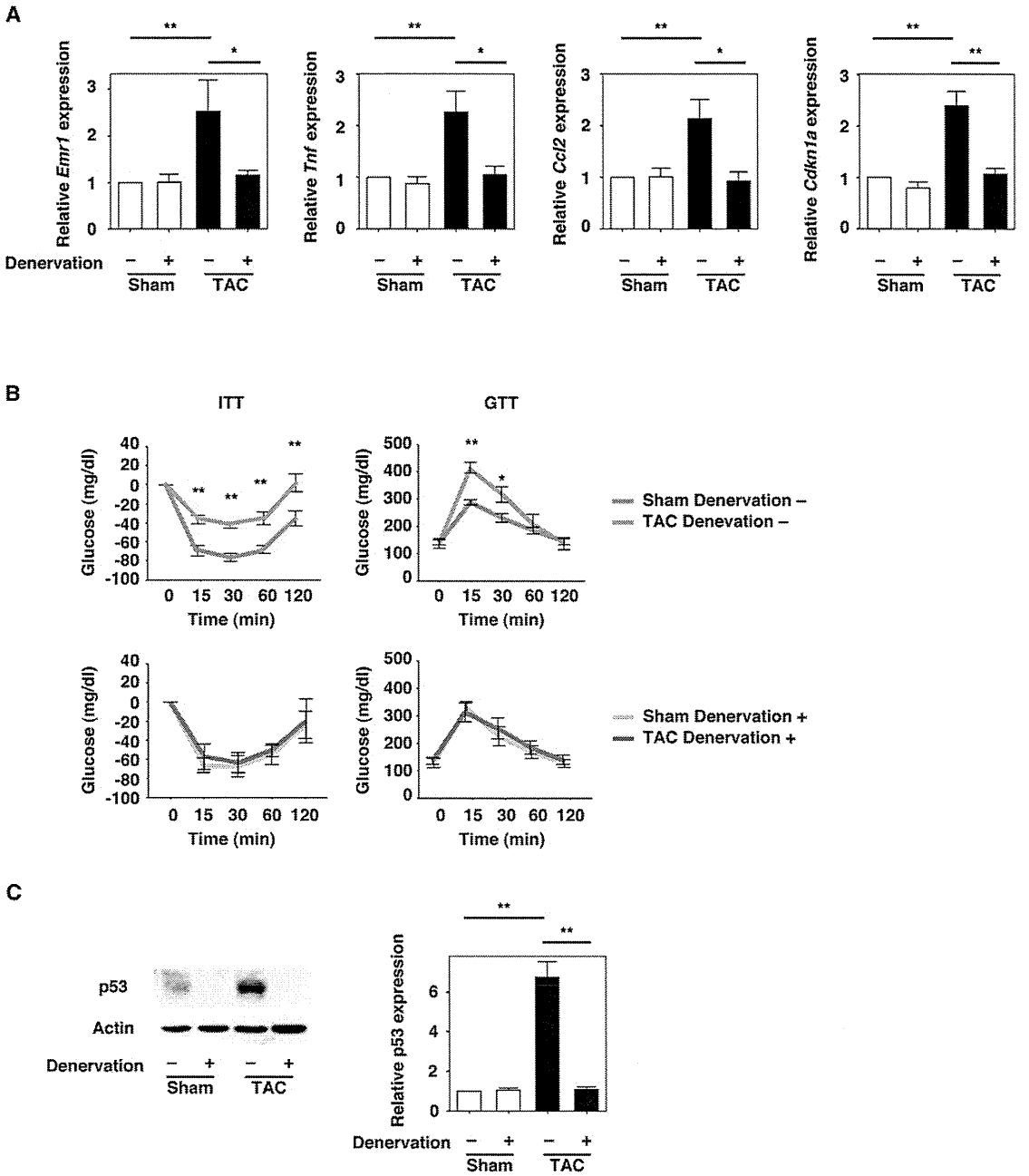

Figure 3. Surgical Transection of the Sympathetic Nerves Attenuates Adipose Tissue Inflammation and Systemic Insulin Resistance

(A) Real-time PCR assessing the expression of *Emr1*, *Tnf* (Tnfα), *Ccl2* (MCP1), and *Cdkn1a* (p21) levels in adipose tissues of mice at 6 weeks after sham operation (Sham) or TAC with or without surgical transection of the sympathetic nerves (Denervation) of epididymal fat (n = 8).

(B) Insulin tolerance test (ITT) and glucose tolerance test (GTT) of mice at 6 weeks after sham operation (Sham) or TAC with or without surgical denervation (n = 20).

(C) Western blot analysis of p53 in adipose tissues of mice at 6 weeks after sham operation (Sham) or TAC with or without surgical denervation. The right graph indicates the quantitative data on p53 expression (n = 3). Data are shown as the means ± S.E.M. *p < 0.05, **p < 0.01.

tissue p53 expression and inflammation (Figures S5H–S5J). Inhibition of p53 activation in adipose tissue by genetic disruption significantly attenuated inflammation of this tissue and improved metabolic abnormalities (Figures S5K and S5L). These results suggest that the same mechanism underlies insulin resistance associated with heart failure due to both pressure overload and MI.

Influence of Inhibiting p53-Induced Adipose Tissue Inflammation on Cardiac Function

To investigate whether inhibition of p53-induced adipose tissue inflammation could influence cardiac function in the development of heart failure, we performed TAC and monitored cardiac function in adipo-p53 KO mice. We found that adipo-p53 KO mice showed significantly better cardiac function and less LV

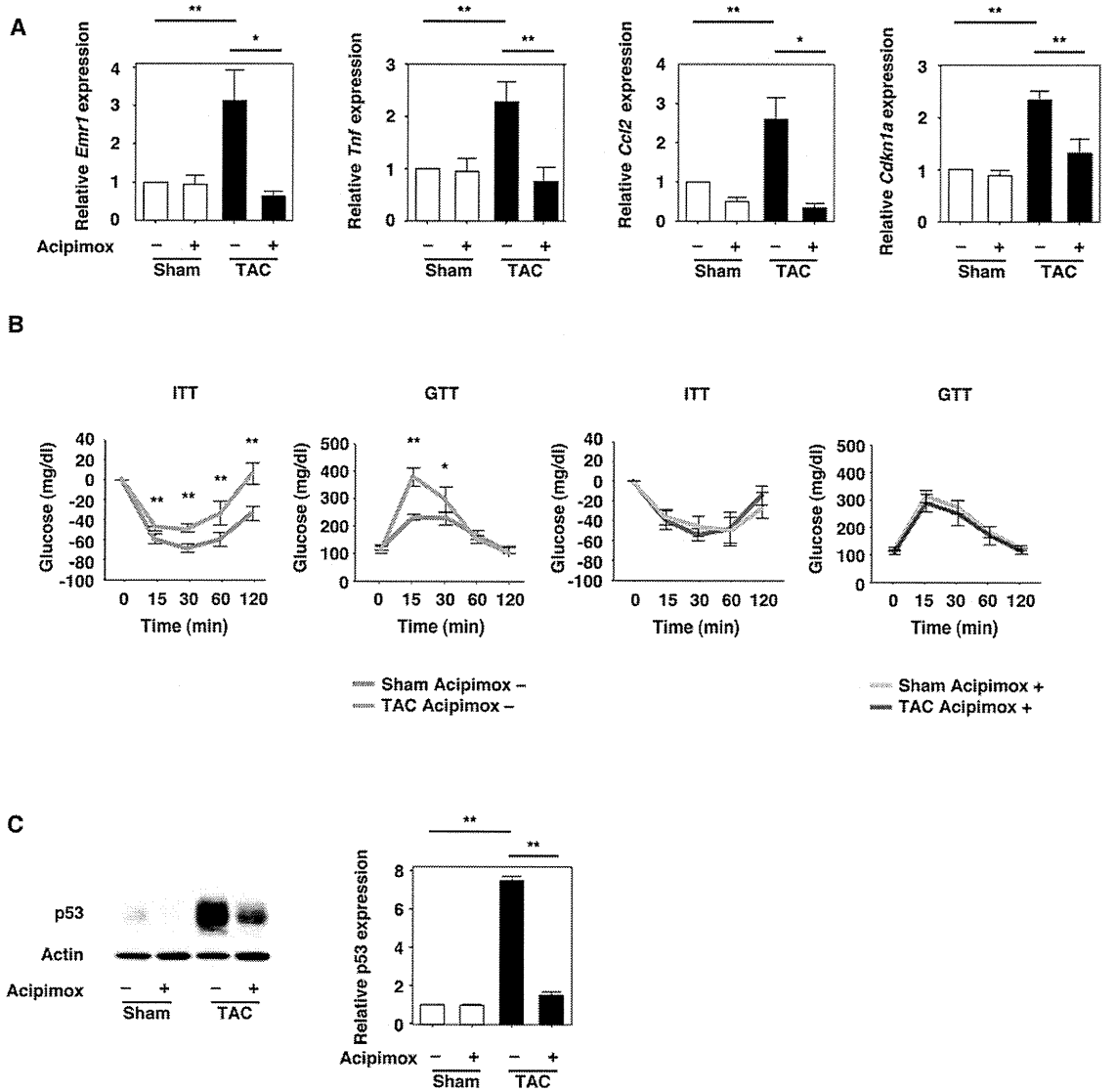

Figure 4. Treatment with a Lipolysis Inhibitor Ameliorates Adipose Tissue Inflammation and Systemic Insulin Resistance

(A) Real-time PCR assessing the expression of *Emr1*, *Tnf* (Tnfα), *Ccl2* (MCP1), and *Cdkn1a* (p21) levels in adipose tissue of mice at 6 weeks after sham operation (Sham) or TAC with or without acipimox treatment (n = 8).

(B) Insulin tolerance test (ITT) and glucose tolerance test (GTT) of mice at 6 weeks after sham operation (Sham) or TAC with or without acipimox treatment (n = 32).

(C) Western blot analysis of p53 in adipose tissues of mice at 6 weeks after sham operation (Sham) or TAC with or without acipimox treatment. Actin was used as an equal loading control. The right graph indicates the quantitative data on p53 expression (n = 3). Data are shown as the means ± S.E.M. *p < 0.05, **p < 0.01.

enlargement compared with their littermate controls (Figure 6A). They also showed better survival during the chronic phase of heart failure (Figure 6B). Similar results were observed in another model of heart failure induced by MI (Figure S6A). Furthermore, administration of a p53 inhibitor (pifithrin-α) into the adipose tissue of the TAC or MI model mice after the onset of heart failure improved cardiac dysfunction, as well as adipose tissue inflammation, and metabolic abnormalities (Figures 6C–6E and S6B–S6D), indicating that inhibition of p53 may be useful for the treatment of heart failure and its associated metabolic abnormalities. Moreover, we noted significant improvement of cardiac function after sympathetic nerve blockade (Figures S6E and S6F). However, treatment of TAC mice with acipimox was found to exacerbate cardiac dysfunction (Figure S6G), presumably because it impaired fatty acid metabolism and energy production in cardiomyocytes, as reported previously (Tuunanen et al., 2006).

Mechanism of p53-Induced Adipose Tissue Inflammation during Heart Failure

Because our results indicated that adrenergic activation induced lipolysis that upregulated p53 and promoted adipose tissue inflammation, we speculated that an excess of fatty acids might be involved in the upregulation of p53 in adipose tissue. Therefore, we examined the effect of palmitic acid on cultured preadipocytes. Treatment with palmitic acid significantly increased the

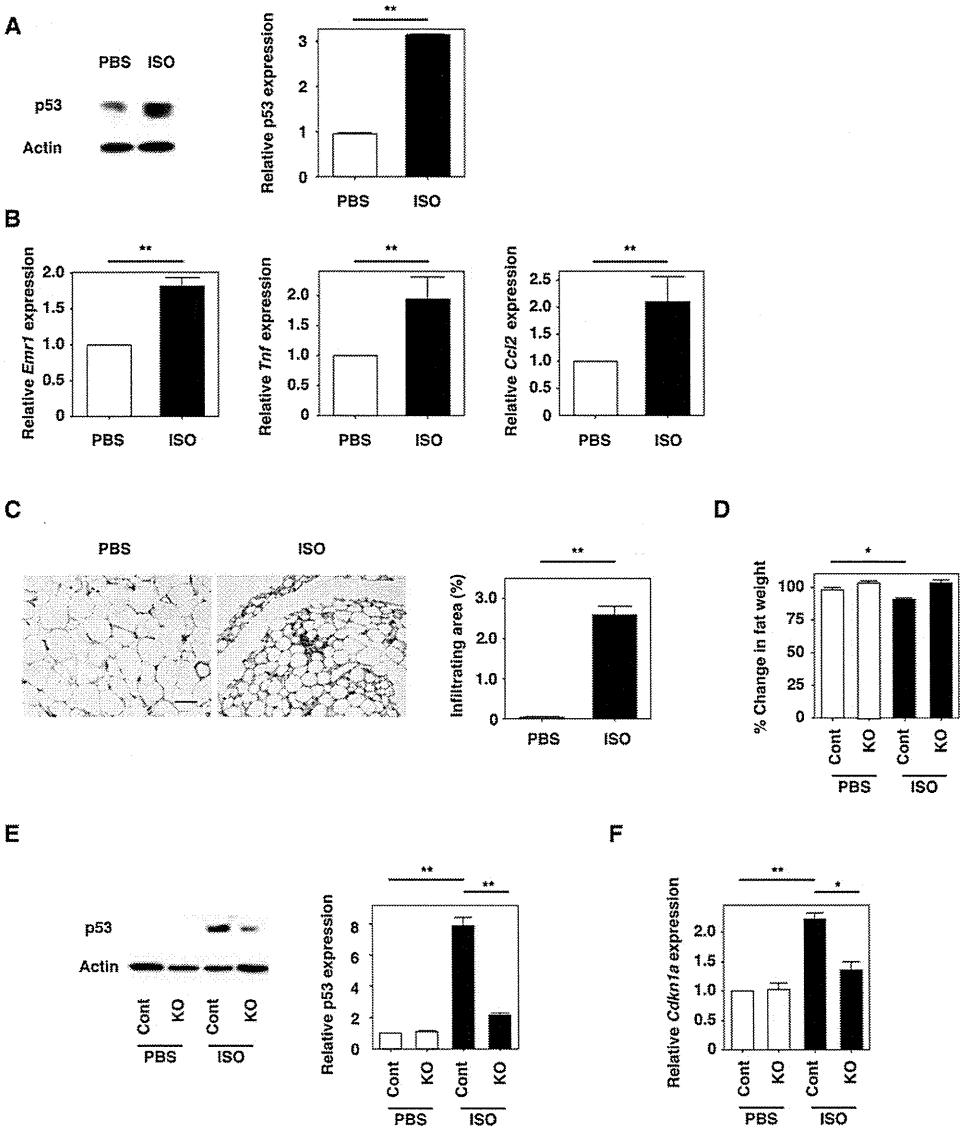

Figure 5. Role of Lipolysis in the Regulation of Adipose p53 Expression and Inflammation

(A) Western blot analysis of p53 in adipose tissues of wild-type mice treated with PBS or isoproterenol (ISO). Actin was used as an equal loading control. The right graph indicates the quantitative data on p53 expression (n = 3).

(B) Real-time PCR assessing the expression of *Emr1*, *Tnf* (Tnfα), and *Ccl2* (MCP1) levels in adipose tissues of wild-type mice treated with PBS or isoproterenol (ISO) (n = 8).

(C) Hematoxylin and eosin staining of adipose tissues of wild-type mice treated with PBS or isoproterenol (ISO). Scale bar, 50 μm. The right graph indicates the quantitative data on macrophage infiltration (n = 4).

(D) The changes in weight of adipose tissues isolated from Atgl-deficient mice (KO) and littermate controls (Cont) after treatment with PBS or isoproterenol (ISO) (n = 6).

(E) Expression of p53 was examined in adipose tissues of Atgl-deficient mice (KO) and littermate controls (Cont) treated with PBS or isoproterenol (ISO) by western blot analysis. The right graph indicates the quantitative data on p53 expression (n = 3).

(F) Real-time PCR assessing the expression of *Cdkn1a* (p21) level in adipose tissues isolated from Atgl-deficient mice (KO) and littermate controls (Cont) after treatment with PBS or isoproterenol (ISO) (n = 6). Data are shown as the means ± S.E.M. *$p < 0.05$, **$p < 0.01$.

intracellular level of reactive oxygen species (ROS) and caused DNA damage, as demonstrated by the increase of γH2AX, which in turn upregulated p53 expression (Figures 7A–7C, S7A, and S7B). This upregulation of p53 was associated with an increase of NF-κB activity and proinflammatory cytokine expression (Figures 7D and 7E). Because it has been reported that p53 enhances the activity of NF-κB, which regulates various cytokines including *TNF-α* and *CCL2* (Benoit et al., 2006; Ryan et al., 2000), we examined the relationship between p53 expression and NF-κB activation. We demonstrated that the disruption of p53 expression significantly attenuated palmitic acid-induced activation of NF-κB and upregulation of *Ccl2*

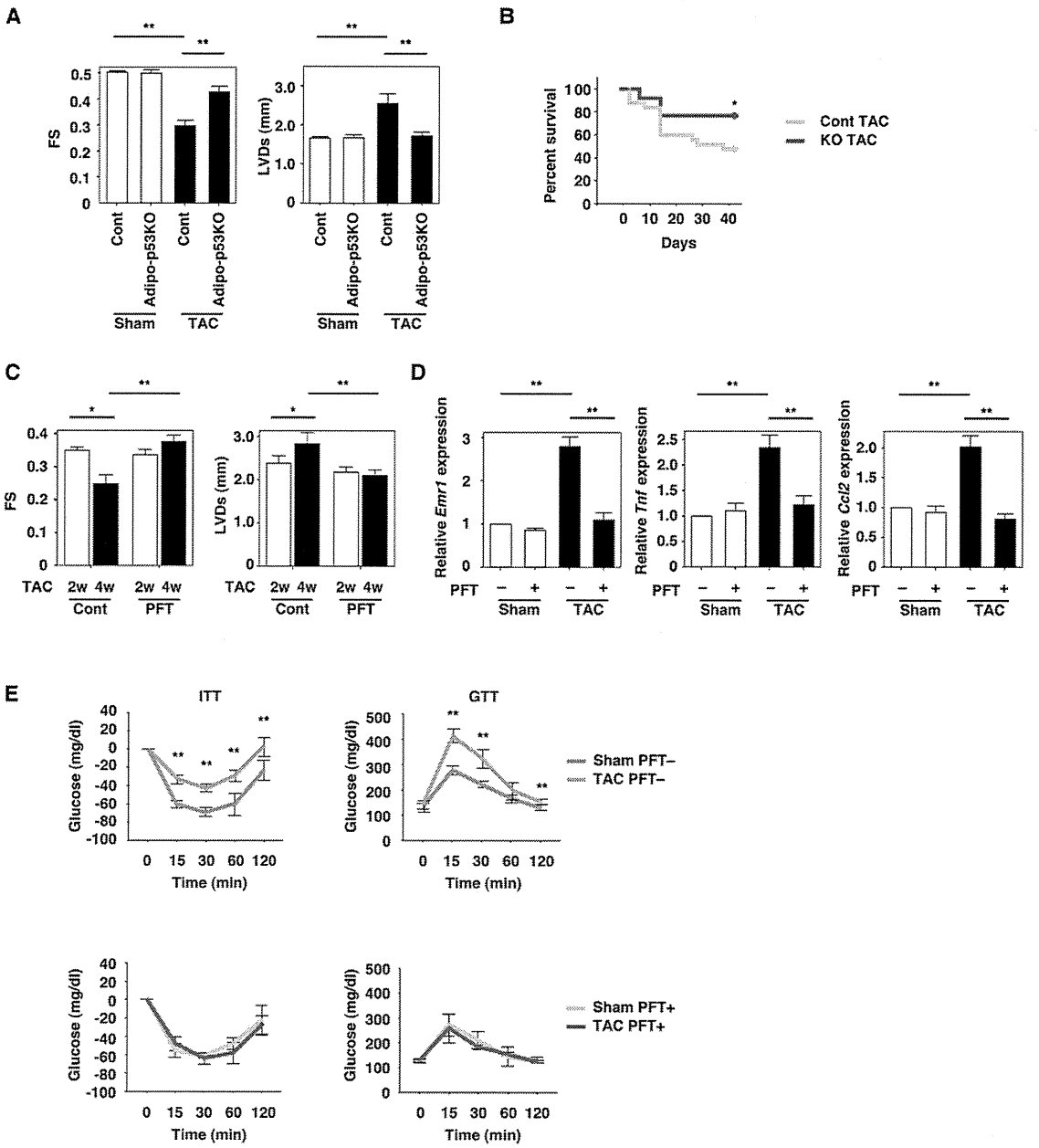

Figure 6. Influence of Inhibiting p53-Induced Adipose Tissue Inflammation on Cardiac Function

(A) Echocardiography to assess systolic function (FS) and ventricular size (LVDs) in adipocyte-specific p53-deficient mice (adipo-p53 KO) and littermate controls (Cont) at 6 weeks after sham operation or TAC (n = 8). FS, fractional shortening; LVDs, left ventricular end-systolic diameter.

(B) Survival rate of adipocyte-specific p53-deficient mice (adipo-p53 KO) and littermate controls (Cont) after TAC procedure (n = 25).

(C) Pifithrin-α (PFT) was administered into the adipose tissue of mice at 2–4 weeks after TAC, and systolic function (FS) and ventricular size (LVDs) were estimated before (2w, 2 weeks after TAC) and after (4w, 4 weeks after TAC) treatment by echocardiography (n = 5).

(D) Real-time PCR assessing the expression of *Emr1*, *Tnf* (Tnfα), and *Ccl2* (MCP1) levels in adipose tissue of mice at 4 weeks after sham operation or TAC with or without pifithrin-α (PFT) treatment (n = 4).

(E) Insulin tolerance test (ITT) and glucose tolerance test (GTT) of mice at 4 weeks after sham operation or TAC with or without pifithrin-α (PFT) treatment (n = 12).

Data are shown as the means ± S.E.M. *p < 0.05, **p < 0.01.

(Figures 7D and 7E), whereas knockdown of the NF-κB component p50 markedly inhibited palmitic acid-induced upregulation of *Ccl2* (Figure 7E). In addition, treatment with an antioxidant inhibited palmitic acid-induced DNA damage and upregulation of p53 (Figures S7A and S7B). We also found that ROS and γH2AX expression were increased in the adipose tissue of mice with heart failure (Figures 7F and 7G). Furthermore, nuclear localization of p50 was enhanced in adipose tissue during heart failure (Figures 7H and S7C). This increase of nuclear p50 expression and the upregulation of proinflammatory cytokines

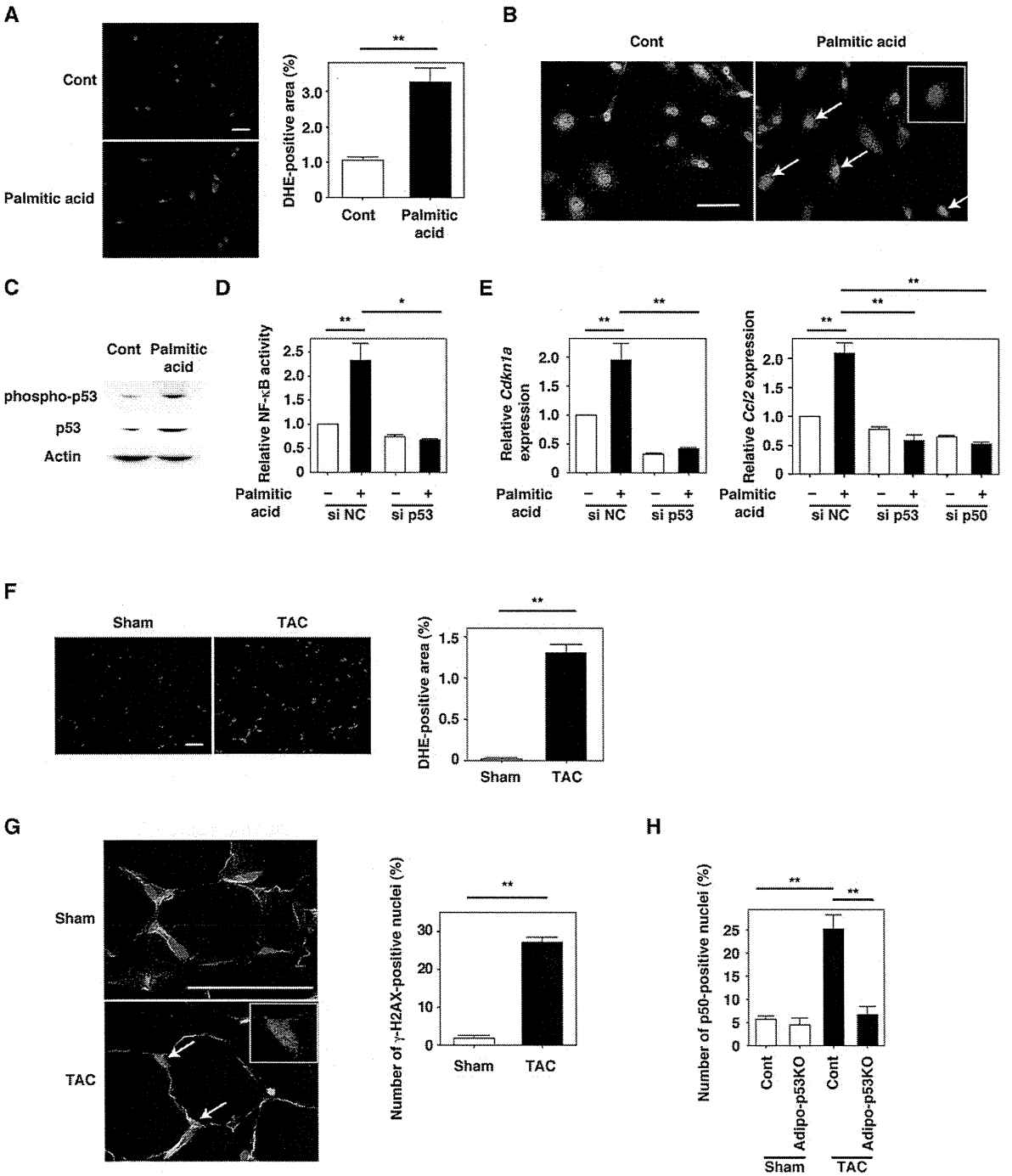

Figure 7. Mechanism of p53-Induced Adipose Tissue Inflammation during Heart Failure

(A) Dihydroethidium (DHE) staining (red) of preadipocytes treated with vehicle (Cont) or palmitic acid (500 μM) for 10 min. Nuclei were stained with Hoechst dye (blue). Scale bar indicates 50 μm. The right graph indicates the quantitative data on DHE-positive area (n = 4).

(B) Immunofluorescent staining for γ-H2AX (red) in preadipocytes treated with vehicle (Cont) or palmitic acid (500 μM) for 1 hr. Nuclei and plasma membranes were stained with Hoechst dye (blue) and Wheat Germ agglutinin lectin (green). Scale bar indicates 50 μm.

(C) Western blot analysis of phospho-p53 and p53 expression in preadipocytes treated with vehicle (Cont) or palmitic acid (500 μM).

(D) Small-interfering RNA targeting p53 (sip53) or negative control RNA (siNC) was introduced into preadipocytes treated with or without palmitic acid (500 μM) for 12 hr. The NF-κB activity was examined by luciferase assay (n = 5).

(E) Real-time PCR assessing the expression of *Cdkn1a* (p21) and *Ccl2* (MCP1) levels in preadipocytes prepared in Figure 7D (n = 9). The effect of small-interfering RNA targeting the NF-κB component p50 (sip50) on the expression of *Ccl2* (MCP1) was also examined (n = 9).

(F) Dihydroethidium (DHE) staining (red) in adipose tissue from sham-operated (Sham) and TAC mice. Nuclei were stained with Hoechst dye (blue). Scale bar indicates 20 μm. The right graph indicates the quantitative data on DHE-positive area (n = 5).

were inhibited by disruption of p53 in adipose tissue (Figures 2B, 7H, and S7C). Moreover, treatment with a lipolysis inhibitor significantly inhibited the heart failure-induced increase of ROS and nuclear p50 expression (Figures S7D and S7E). Inhibition of NF-κB activation in adipose tissue by BAY 11-7082 also significantly attenuated adipose tissue inflammation and improved metabolic abnormalities and cardiac dysfunction in TAC mice (Figures S7F–S7H). These results indicate that adrenergic activation by heart failure induces lipolysis in adipose tissue, which increases DNA damage due to ROS and thus upregulates p53. Activation of p53 then induces adipose tissue inflammation and metabolic abnormalities by upregulating the expression of NF-κB-dependent proinflammatory cytokines.

DISCUSSION

Although treatments that achieve neurohumoral antagonism have successfully reduced the morbidity and mortality of heart failure, the death rate remains unacceptably high (Kannel, 2000). Various metabolic abnormalities are associated with heart failure, and recent data have suggested that heart failure itself promotes adverse changes of metabolism, such as systemic insulin resistance (Ashrafian et al., 2007; Witteles and Fowler, 2008). Thus, a detrimental vicious cycle may be postulated, in which heart failure induces insulin resistance that in turn accelerates cardiac dysfunction (Opie, 2004). However, studies on the molecular mechanisms of such metabolic abnormalities in heart failure are largely preliminary and the results have sometimes been conflicting. In the present study, we demonstrated a causal role for heart failure in the development of insulin resistance by using two mouse models of heart failure, and we elucidated the underlying mechanisms. We found that the hyperadrenergic state of heart failure initiated a vicious metabolic cycle by promoting lipolysis in adipose tissue that increased the release of free fatty acids and upregulated p53 expression and proinflammatory cytokine production in adipose tissue, which then promoted systemic insulin resistance. Cardiac insulin resistance is considered to contribute to the development of heart failure. Because excessive cardiac insulin signaling has been reported to exacerbate systolic dysfunction in both TAC and MI models (Shimizu et al., 2010), hyperinsulinemia associated with systemic insulin resistance may also have a pathological role in heart failure until insulin resistance becomes evident in the myocardium. Inhibition of lipolysis by sympathetic denervation or by treatment with a lipolysis inhibitor improved insulin resistance in our heart failure model. Plasma free fatty acid levels were significantly elevated after the onset of heart failure, whereas this increase was attenuated by inhibition of lipolysis with acipimox, denervation, or guanethidine. Disruption of p53 in adipose tissue also markedly attenuated adipose inflammation and metabolic abnormalities associated with heart failure, whereas fatty acid levels were unaffected. Thus, adipose tissue inflammation rather than the increase of plasma free fatty acids per se is involved in the impairment of insulin sensitivity and glucose tolerance associated with heart failure. We also noted that p53 was modestly upregulated in the liver and skeletal muscle, presumably due to the increase of circulating free fatty acids. However, we did not detect a strong inflammatory response in those tissues under our experimental conditions (I. Shimizu and T. Minamino, unpublished data), suggesting that upregulation of adipose tissue p53 is more important for the development of metabolic abnormalities during heart failure. This concept is further supported by our finding that disruption of p53 activation in adipose tissue nearly normalized insulin resistance and glucose intolerance provoked by heart failure.

We observed that systolic cardiac function and survival with chronic heart failure were significantly better for adipo-p53 KO mice than their control littermates. Suppression of p53 activity in adipose tissue by administration of a p53 inhibitor after the onset of heart failure improved cardiac dysfunction and also reduced adipose tissue inflammation and metabolic abnormalities in both the TAC and MI models. Inhibition of NF-κB activity in adipose tissue also improved cardiac dysfunction, as well as adipose tissue inflammation and insulin resistance. Improvement of cardiac dysfunction by disruption of p53 in adipose tissue was not associated with a decrease of plasma free fatty acid levels. Systemic inhibition of lipolysis (Atgl deficiency or acipimox treatment) and disturbance of lipolysis in adipose tissue (denervation or guanethidine treatment) significantly reduced plasma free fatty acid levels (Haemmerle et al., 2006). However, the former intervention accelerated heart failure, whereas cardiac dysfunction was improved by the latter. Thus, the beneficial effect of inhibiting p53-induced adipose tissue inflammation on cardiac function is independent of changes in circulating free fatty acid levels, and lipolysis in cardiomyocytes appears to have a crucial role in cardiac metabolism and energy production. Although there is evidence suggesting that p53 has a protective role against damage due to ROS and lipotoxicity (Bazuine et al., 2009), our results indicate that chronic activation of p53 in adipose tissue causes inflammation and that inhibition of p53-induced adipose tissue inflammation is a potential target for treating metabolic abnormalities and systolic dysfunction in patients with heart failure.

Adipose tissue was traditionally considered to be a simple energy storage organ, but it is now appreciated that it also has endocrine functions and secretes a variety of factors referred to as adipokines (Donath and Shoelson, 2011; Hotamisligil, 2006; Ouchi et al., 2011). With high calorie intake, the size and number of adipocytes increase, and hypertrophic adipocytes shift the balance toward production of proinflammatory adipokines. This shift in the adipokine profile causes the modification of adipose tissue macrophages from the anti-inflammatory M2 type to the proinflammatory M1 type, and further increases the production of proinflammatory molecules, which in turn

(G) The number of γ-H2AX-positive nuclei (white arrows and inset) in adipose tissue of mice at 6 weeks after sham operation (Sham) or TAC procedure was estimated by immunofluorescent staining for γ-H2AX (red) (n = 5). Nuclei and plasma membranes were stained with Hoechst dye (blue) and Wheat Germ agglutinin lectin (green). Scale bar indicates 50 μm.

(H) The number of p50-positive nuclei in adipose tissue of adipocyte-specific p53-deficient mice (adipo-p53 KO) and littermate controls (Cont) at 6 weeks after sham operation (Sham) or TAC procedure was estimated by immunofluorescent staining for p50 (n = 6). Data are shown as the means ± S.E.M. *$p < 0.05$, **$p < 0.01$.

accelerates the recruitment of activated macrophages into inflamed fatty tissue. Adipokines produced by inflamed adipose tissue have been suggested to play a crucial role in the regulation of glucose and lipid metabolism and to contribute to the development of diabetes (Donath and Shoelson, 2011; Hotamisligil, 2006; Ouchi et al., 2011). It has been reported that excessive calorie intake leads to accumulation of ROS in adipose tissue and subsequently causes DNA damage that activates p53 (Minamino et al., 2009). In contrast to obesity, heart failure decreases body fat tissue mass by inducing lipolysis. Accelerated lipolysis and a subsequent increase of free fatty acids are likely to cause p53 activation because we found that the promotion of lipolysis by treatment with isoproterenol upregulated adipose tissue expression of p53, whereas inhibition of lipolysis by acipimox or disruption of lipase activity attenuated p53 expression. These results are consistent with a recent report describing that fasting-induced lipolysis promotes an immune response in murine adipose tissue (Kosteli et al., 2010). Various molecular mechanisms of p53 activation by heart failure may be postulated, including hypoxia, increased oxidative stress, and induction of endoplasmic reticulum stress (Harris and Levine, 2005; Schenk et al., 2008). Our in vitro and in vivo studies have indicated that an increase of free fatty acids causes ROS-induced DNA damage that upregulates p53 in adipose tissue. Activation of p53 then upregulates the expression of proinflammatory adipokines via the NF-κB signaling pathway and promotes systemic insulin resistance.

The β-blockers are competitive antagonists of β-adrenergic receptors. At one time, β-blockers were contraindicated in patients with heart failure due to their negative inotropic effect. However, several large-scale clinical trials demonstrated the efficacy of β-blockers for reducing morbidity and mortality in heart failure patients with impaired systolic function, so β-blockers are now recommended as first-line agent for these patients (Hjalmarson et al., 2000; Leizorovicz et al., 2002; Packer et al., 2001, 2002). A reduction of heart rate due to inhibition of cardiac β_1-adrenergic receptors is believed to be responsible for most of the therapeutic benefits associated with β-blocker treatment, although this is not the only mechanism of action that may be important in heart failure. It is interesting that treatment with a nonselective β-blocker (carvedilol) achieved a more marked improvement of survival in patients with chronic heart failure than treatment with a β_1-selective blocker (metoprolol) (Poole-Wilson et al., 2003), whereas new-onset diabetes was frequent in heart failure patients during treatment with the β_1-selective blocker (Torp-Pedersen et al., 2007). It has been reported that carvedilol antagonizes the β_3-adrenergic receptor as well as the $\beta_{1/2}$-adrenergic receptors (Schnabel et al., 2000). Taking our results together with these reports, it seems that inhibition of β_3-adrenergic activity in adipose tissue partially accounts for the better clinical outcome in patients treated with this nonselective β-blocker. Recent evidence has suggested that treatment with insulin sensitizers improves systolic function of the failing heart in animal models (Asakawa et al., 2002; Nemoto et al., 2005) but such treatment increases the incidence of heart failure in diabetic patients, presumably because of sodium retention (Home et al., 2009). Inhibition of p53-induced adipose tissue inflammation could be an alternative therapeutic target to block the metabolic vicious cycle in patients with heart failure.

EXPERIMENTAL PROCEDURES

Animal Models

All animal study protocols were approved by the Chiba University review board. C57BL/6 mice were purchased from the SLC Japan (Shizuoka, Japan). TAC and MI were performed in 11-week-old male mice as described previously (Harada et al., 2005; Sano et al., 2007). Sham-operated mice underwent the same procedure except for aortic constriction. Mice that expressed Cre recombinase in adipocytes (Fabp4-Cre) were purchased from Jackson Laboratories. We then crossed Fabp4-Cre mice (with a C57BL/6 background) with mice that carried floxed *Trp53* alleles with a C57BL/6 background (Marino et al., 2000) to generate adipocyte-specific p53 knockout mice. The genotype of littermate controls was Fabp4-Cre$^-$ *Trp53* $^{flox/flox}$. The generation and genotyping of Atgl-deficient mice has been described previously (Haemmerle et al., 2006). Surgical or chemical denervation was performed before TAC operation as described previously (Demas and Bartness, 2001; Foster and Bartness, 2006), with slight modification. In brief, the epididymal fat pad was gently separated from the skin and the abdominal wall by using a dissecting microscope. For surgical denervation, a drop of 1% toluidine blue was applied to the fat pad to facilitate visualization of the nerves. The nerves were then freed from the surrounding tissue and vasculature and cut in two or more locations, and the segments were removed to prevent possible reconnection. Chemical denervation was performed by the local injection of guanethidine sulfate (400 μg, Santa Cruz) into bilateral epididymal fat. Sham-operated mice for surgical denervation underwent the same procedure except for transection of the nerve. For the control group for chemical denervation, saline was injected into adipose tissue rather than guanethidine. Acipimox (Sigma) were provided in drinking water (at a concentration of 0.05%) for 6 weeks after TAC operation as described previously (Guo et al., 2009). Isoproterenol (30 mg/kg/day, Sigma) were delivered by infusion pump (DURECT Corporation) for 2 weeks as described previously (Iaccarino et al., 1999). The local injection of pifithrin-α (2.2 mg/kg/week, Carbiochem) or BAY 11-7082 (20 mg/kg/week, Carbiochem) into bilateral epididymal fat was performed to inhibit adipose p53 or NF-κB activity, respectively, from 2 weeks to 4 weeks after operation.

Physiological and Histological Analyses

Echocardiography was performed with a Vevo 770 High Resolution Imaging System (Visual Sonics Inc, Toronto, Ontario, Canada). To minimize variation of the data, the heart rate was always approximately 550–650 beats per minute when cardiac function was assessed. Epididymal fat samples were harvested and fixed in 10% formalin overnight. The samples were embedded in paraffin and sectioned (Narabyouri research Co., Ltd). The sections were subjected to immunohistochemistry or HE staining. The antibodies used are Mac3-specific primary antibody (PharMingen) for macrophages, p50-specific primary antibody (Cell signaling), and phospho-H2AX-specific antibody (Cell signaling).

Laboratory Tests

For the intraperitoneal glucose tolerance test (IGTT), mice were starved for 6 hr and were given glucose intraperitoneally at a dose of 2 g / kg (body weight) in the early afternoon. For the insulin tolerance test, mice were given human insulin intraperitoneally (1 U / kg body weight) at 1:00 pm without starvation. Blood glucose levels were measured with a glucose analyzer (Roche Diagnostics). We analyzed free fatty acid (Biovision, Inc) and norepinephrine levels (LDN) by using ELISA-based immunoassay kits according to the manufacturer's instruction.

Western Blot Analysis

The lysates were resolved by SDS-polyacrylamide gel electrophoresis. Proteins were transferred to a polyvinylidene difluoride membrane (Millipore, Bedford, MA), which was incubated with the primary antibody followed by anti-rabbit or anti-mouse immunoglobulin-G conjugated with horseradish peroxidase (Jackson, West Grove, PA).

Cell Culture

Human preadipocytes were purchased from Sanko (Tokyo, Japan) and were cultured according to the manufacturer's instructions. NIH 3T3-L1 cells were cultured in high-glucose DMEM plus 10% fetal bovine serum.

Ex Vivo Culture

Epididymal fat was extracted from Atgl-deficient or littermate mice at 17 weeks of age. Freshly isolated fat pads (100–120 mg) were incubated in Dulbecco's modified Eagle's medium supplemented with 10% fetal bovine serum in the presence of isoproterenol (10 μM) for 48 hr. Fat pads were treated with PBS instead of isoproterenol in the control group.

Statistical Analysis

Data are shown as the mean ± SEM. Differences between groups were examined by Student's t-test or ANOVA followed by Bonferroni's correction for comparison of means. For survival analysis, the Kaplan-Meier method and log-rank test were used. For all analyses, $p < 0.05$ was considered statistically significant.

SUPPLEMENTAL INFORMATION

Supplemental Information includes Supplemental Experimental Procedures and seven figures and can be found with this article online at doi:10.1016/j.cmet.2011.12.006.

ACKNOWLEDGMENTS

We thank A. Berns (The Netherlands Cancer Institute) for floxed p53 mice, T. Fujita (The Tokyo Metropolitan Institute of Medical Science) for reagents, and E .Takahashi, M. Iijima, and I. Sakamoto for their excellent technical assistance. This work was supported by a Grant-in-Aid for Scientific Research from the Ministry of Education, Culture, Sports, Science and Technology of Japan and grants from the Ono Medical Research Foundation; the Uehara Memorial Foundation; the Daiichi-Sankyo Foundation of Life Science; the NOVARTIS Foundation for the Promotion Science; the Japan Diabetes Foundation; the Mitsui Life Social Welfare Foundation; the Naito Foundation; the Japanese Society of Anti-Aging Medicine; and the Mitsubishi Pharma Research Foundation (to T.M.); a Grant-in-Aid for Scientific Research from the Ministry of Education, Science, Sports, and Culture and Health and Labor Sciences Research Grants (to I.K.); and a Grant-in-Aid for Scientific Research from the Ministry of Education, Science, Sports, and Culture, and Health and a grant from the Uehara Memorial Foundation, Takeda Science Foundation, and Kowa Life Science Foundation (to I.S.).

Received: June 10, 2011
Revised: October 27, 2011
Accepted: December 9, 2011
Published online: January 3, 2012

REFERENCES

Arnlöv, J., Lind, L., Zethelius, B., Andrén, B., Hales, C.N., Vessby, B., and Lithell, H. (2001). Several factors associated with the insulin resistance syndrome are predictors of left ventricular systolic dysfunction in a male population after 20 years of follow-up. Am. Heart J. *142*, 720–724.

Asakawa, M., Takano, H., Nagai, T., Uozumi, H., Hasegawa, H., Kubota, N., Saito, T., Masuda, Y., Kadowaki, T., and Komuro, I. (2002). Peroxisome proliferator-activated receptor gamma plays a critical role in inhibition of cardiac hypertrophy in vitro and in vivo. Circulation *105*, 1240–1246.

Ashrafian, H., Frenneaux, M.P., and Opie, L.H. (2007). Metabolic mechanisms in heart failure. Circulation *116*, 434–448.

Bazuine, M., Stenkula, K.G., Cam, M., Arroyo, M., and Cushman, S.W. (2009). Guardian of corpulence: a hypothesis on p53 signaling in the fat cell. Clin. Lipidol. *4*, 231–243.

Benoit, V., de Moraes, E., Dar, N.A., Taranchon, E., Bours, V., Hautefeuille, A., Tanière, P., Chariot, A., Scoazec, J.Y., de Moura Gallo, C.V., et al. (2006). Transcriptional activation of cyclooxygenase-2 by tumor suppressor p53 requires nuclear factor-kappaB. Oncogene *25*, 5708–5718.

Demas, G.E., and Bartness, T.J. (2001). Novel method for localized, functional sympathetic nervous system denervation of peripheral tissue using guanethidine. J. Neurosci. Methods *112*, 21–28.

Donath, M.Y., and Shoelson, S.E. (2011). Type 2 diabetes as an inflammatory disease. Nat. Rev. Immunol. *11*, 98–107.

Edwards, M.G., Anderson, R.M., Yuan, M., Kendziorski, C.M., Weindruch, R., and Prolla, T.A. (2007). Gene expression profiling of aging reveals activation of a p53-mediated transcriptional program. BMC Genomics *8*, 80.

Floras, J.S. (2009). Sympathetic nervous system activation in human heart failure: clinical implications of an updated model. J. Am. Coll. Cardiol. *54*, 375–385.

Foster, M.T., and Bartness, T.J. (2006). Sympathetic but not sensory denervation stimulates white adipocyte proliferation. Am. J. Physiol. Regul. Integr. Comp. Physiol. *291*, R1630–R1637.

Guo, W., Wong, S., Pudney, J., Jasuja, R., Hua, N., Jiang, L., Miller, A., Hruz, P.W., Hamilton, J.A., and Bhasin, S. (2009). Acipimox, an inhibitor of lipolysis, attenuates atherogenesis in LDLR-null mice treated with HIV protease inhibitor ritonavir. Arterioscler. Thromb. Vasc. Biol. *29*, 2028–2032.

Haemmerle, G., Lass, A., Zimmermann, R., Gorkiewicz, G., Meyer, C., Rozman, J., Heldmaier, G., Maier, R., Theussl, C., Eder, S., et al. (2006). Defective lipolysis and altered energy metabolism in mice lacking adipose triglyceride lipase. Science *312*, 734–737.

Harada, M., Qin, Y., Takano, H., Minamino, T., Zou, Y., Toko, H., Ohtsuka, M., Matsuura, K., Sano, M., Nishi, J., et al. (2005). G-CSF prevents cardiac remodeling after myocardial infarction by activating the Jak-Stat pathway in cardiomyocytes. Nat. Med. *11*, 305–311.

Harris, S.L., and Levine, A.J. (2005). The p53 pathway: positive and negative feedback loops. Oncogene *24*, 2899–2908.

Hjalmarson, A., Goldstein, S., Fagerberg, B., Wedel, H., Waagstein, F., Kjekshus, J., Wikstrand, J., El Allaf, D., Vítovec, J., Aldershvile, J., et al; MERIT-HF Study Group. (2000). Effects of controlled-release metoprolol on total mortality, hospitalizations, and well-being in patients with heart failure: the Metoprolol CR/XL Randomized Intervention Trial in congestive heart failure (MERIT-HF). JAMA *283*, 1295–1302.

Home, P.D., Pocock, S.J., Beck-Nielsen, H., Curtis, P.S., Gomis, R., Hanefeld, M., Jones, N.P., Komajda, M., and McMurray, J.J.; RECORD Study Team. (2009). Rosiglitazone evaluated for cardiovascular outcomes in oral agent combination therapy for type 2 diabetes (RECORD): a multicentre, randomised, open-label trial. Lancet *373*, 2125–2135.

Hotamisligil, G.S. (2006). Inflammation and metabolic disorders. Nature *444*, 860–867.

Hotamisligil, G.S., Shargill, N.S., and Spiegelman, B.M. (1993). Adipose expression of tumor necrosis factor-alpha: direct role in obesity-linked insulin resistance. Science *259*, 87–91.

Iaccarino, G., Dolber, P.C., Lefkowitz, R.J., and Koch, W.J. (1999). Bbeta-adrenergic receptor kinase-1 levels in catecholamine-induced myocardial hypertrophy: regulation by beta- but not alpha1-adrenergic stimulation. Hypertension *33*, 396–401.

Ingelsson, E., Sundström, J., Arnlöv, J., Zethelius, B., and Lind, L. (2005). Insulin resistance and risk of congestive heart failure. JAMA *294*, 334–341.

Kamei, N., Tobe, K., Suzuki, R., Ohsugi, M., Watanabe, T., Kubota, N., Ohtsuka-Kowatari, N., Kumagai, K., Sakamoto, K., Kobayashi, M., et al. (2006). Overexpression of monocyte chemoattractant protein-1 in adipose tissues causes macrophage recruitment and insulin resistance. J. Biol. Chem. *281*, 26602–26614.

Kannel, W.B. (2000). Incidence and epidemiology of heart failure. Heart Fail. Rev. *5*, 167–173.

Kosteli, A., Sugaru, E., Haemmerle, G., Martin, J.F., Lei, J., Zechner, R., and Ferrante, A.W., Jr. (2010). Weight loss and lipolysis promote a dynamic immune response in murine adipose tissue. J. Clin. Invest. *120*, 3466–3479.

Leizorovicz, A., Lechat, P., Cucherat, M., and Bugnard, F. (2002). Bisoprolol for the treatment of chronic heart failure: a meta-analysis on individual data of two placebo-controlled studies—CIBIS and CIBIS II. Cardiac Insufficiency Bisoprolol Study. Am. Heart J. *143*, 301–307.

Lopaschuk, G.D., Folmes, C.D., and Stanley, W.C. (2007). Cardiac energy metabolism in obesity. Circ. Res. *101*, 335–347.

Maier, B., Gluba, W., Bernier, B., Turner, T., Mohammad, K., Guise, T., Sutherland, A., Thorner, M., and Scrable, H. (2004). Modulation of mammalian life span by the short isoform of p53. Genes Dev. *18*, 306–319.

Marino, S., Vooijs, M., van Der Gulden, H., Jonkers, J., and Berns, A. (2000). Induction of medulloblastomas in p53-null mutant mice by somatic inactivation of Rb in the external granular layer cells of the cerebellum. Genes Dev. *14*, 994–1004.

Meek, D.W. (2009). Tumour suppression by p53: a role for the DNA damage response? Nat. Rev. Cancer *9*, 714–723.

Minamino, T., and Komuro, I. (2007). Vascular cell senescence: contribution to atherosclerosis. Circ. Res. *100*, 15–26.

Minamino, T., and Komuro, I. (2008). Vascular aging: insights from studies on cellular senescence, stem cell aging, and progeroid syndromes. Nat. Clin. Pract. Cardiovasc. Med. *5*, 637–648.

Minamino, T., Orimo, M., Shimizu, I., Kunieda, T., Yokoyama, M., Ito, T., Nojima, A., Nabetani, A., Oike, Y., Matsubara, H., et al. (2009). A crucial role for adipose tissue p53 in the regulation of insulin resistance. Nat. Med. *15*, 1082–1087.

Nemoto, S., Razeghi, P., Ishiyama, M., De Freitas, G., Taegtmeyer, H., and Carabello, B.A. (2005). PPAR-gamma agonist rosiglitazone ameliorates ventricular dysfunction in experimental chronic mitral regurgitation. Am. J. Physiol. Heart Circ. Physiol. *288*, H77–H82.

Neubauer, S. (2007). The failing heart—an engine out of fuel. N. Engl. J. Med. *356*, 1140–1151.

Nikolaidis, L.A., Sturzu, A., Stolarski, C., Elahi, D., Shen, Y.T., and Shannon, R.P. (2004). The development of myocardial insulin resistance in conscious dogs with advanced dilated cardiomyopathy. Cardiovasc. Res. *61*, 297–306.

Opie, L.H. (2004). The metabolic vicious cycle in heart failure. Lancet *364*, 1733–1734.

Ouchi, N., Parker, J.L., Lugus, J.J., and Walsh, K. (2011). Adipokines in inflammation and metabolic disease. Nat. Rev. Immunol. *11*, 85–97.

Packer, M., Coats, A.J., Fowler, M.B., Katus, H.A., Krum, H., Mohacsi, P., Rouleau, J.L., Tendera, M., Castaigne, A., Roecker, E.B., et al; Carvedilol Prospective Randomized Cumulative Survival Study Group. (2001). Effect of carvedilol on survival in severe chronic heart failure. N. Engl. J. Med. *344*, 1651–1658.

Packer, M., Fowler, M.B., Roecker, E.B., Coats, A.J., Katus, H.A., Krum, H., Mohacsi, P., Rouleau, J.L., Tendera, M., Staiger, C., et al; Carvedilol Prospective Randomized Cumulative Survival (COPERNICUS) Study Group. (2002). Effect of carvedilol on the morbidity of patients with severe chronic heart failure: results of the carvedilol prospective randomized cumulative survival (COPERNICUS) study. Circulation *106*, 2194–2199.

Poole-Wilson, P.A., Swedberg, K., Cleland, J.G., Di Lenarda, A., Hanrath, P., Komajda, M., Lubsen, J., Lutiger, B., Metra, M., Remme, W.J., et al; Carvedilol Or Metoprolol European Trial Investigators. (2003). Comparison of carvedilol and metoprolol on clinical outcomes in patients with chronic heart failure in the Carvedilol Or Metoprolol European Trial (COMET): randomised controlled trial. Lancet *362*, 7–13.

Royds, J.A., and Iacopetta, B. (2006). p53 and disease: when the guardian angel fails. Cell Death Differ. *13*, 1017–1026.

Ryan, K.M., Ernst, M.K., Rice, N.R., and Vousden, K.H. (2000). Role of NF-kappaB in p53-mediated programmed cell death. Nature *404*, 892–897.

Sano, M., Minamino, T., Toko, H., Miyauchi, H., Orimo, M., Qin, Y., Akazawa, H., Tateno, K., Kayama, Y., Harada, M., et al. (2007). p53-induced inhibition of Hif-1 causes cardiac dysfunction during pressure overload. Nature *446*, 444–448.

Schenk, S., Saberi, M., and Olefsky, J.M. (2008). Insulin sensitivity: modulation by nutrients and inflammation. J. Clin. Invest. *118*, 2992–3002.

Schnabel, P., Maack, C., Mies, F., Tyroller, S., Scheer, A., and Böhm, M. (2000). Binding properties of beta-blockers at recombinant beta1-, beta2-, and beta3-adrenoceptors. J. Cardiovasc. Pharmacol. *36*, 466–471.

Sharma, N., Okere, I.C., Duda, M.K., Chess, D.J., O'Shea, K.M., and Stanley, W.C. (2007). Potential impact of carbohydrate and fat intake on pathological left ventricular hypertrophy. Cardiovasc. Res. *73*, 257–268.

Shimizu, I., Minamino, T., Toko, H., Okada, S., Ikeda, H., Yasuda, N., Tateno, K., Moriya, J., Yokoyama, M., Nojima, A., et al. (2010). Excessive cardiac insulin signaling exacerbates systolic dysfunction induced by pressure overload in rodents. J. Clin. Invest. *120*, 1506–1514.

Suskin, N., McKelvie, R.S., Burns, R.J., Latini, R., Pericak, D., Probstfield, J., Rouleau, J.L., Sigouin, C., Solymoss, C.B., Tsuyuki, R., et al. (2000). Glucose and insulin abnormalities relate to functional capacity in patients with congestive heart failure. Eur. Heart J. *21*, 1368–1375.

Tenenbaum, A., Motro, M., Fisman, E.Z., Leor, J., Freimark, D., Boyko, V., Mandelzweig, L., Adler, Y., Sherer, Y., and Behar, S. (2003). Functional class in patients with heart failure is associated with the development of diabetes. Am. J. Med. *114*, 271–275.

Torp-Pedersen, C., Metra, M., Charlesworth, A., Spark, P., Lukas, M.A., Poole-Wilson, P.A., Swedberg, K., Cleland, J.G., Di Lenarda, A., Remme, W.J., and Scherhag, A.; COMET investigators. (2007). Effects of metoprolol and carvedilol on pre-existing and new onset diabetes in patients with chronic heart failure: data from the Carvedilol Or Metoprolol European Trial (COMET). Heart *93*, 968–973.

Tuunanen, H., Engblom, E., Naum, A., Någren, K., Hesse, B., Airaksinen, K.E., Nuutila, P., Iozzo, P., Ukkonen, H., Opie, L.H., and Knuuti, J. (2006). Free fatty acid depletion acutely decreases cardiac work and efficiency in cardiomyopathic heart failure. Circulation *114*, 2130–2137.

Tyner, S.D., Venkatachalam, S., Choi, J., Jones, S., Ghebranious, N., Igelmann, H., Lu, X., Soron, G., Cooper, B., Brayton, C., et al. (2002). p53 mutant mice that display early ageing-associated phenotypes. Nature *415*, 45–53.

Vousden, K.H., and Lane, D.P. (2007). p53 in health and disease. Nat. Rev. Mol. Cell Biol. *8*, 275–283.

Vousden, K.H., and Prives, C. (2009). Blinded by the Light: The Growing Complexity of p53. Cell *137*, 413–431.

Vousden, K.H., and Ryan, K.M. (2009). p53 and metabolism. Nat. Rev. Cancer *9*, 691–700.

Weisberg, S.P., McCann, D., Desai, M., Rosenbaum, M., Leibel, R.L., and Ferrante, A.W., Jr. (2003). Obesity is associated with macrophage accumulation in adipose tissue. J. Clin. Invest. *112*, 1796–1808.

Witteles, R.M., and Fowler, M.B. (2008). Insulin-resistant cardiomyopathy clinical evidence, mechanisms, and treatment options. J. Am. Coll. Cardiol. *51*, 93–102.

Young, M.E., McNulty, P., and Taegtmeyer, H. (2002). Adaptation and maladaptation of the heart in diabetes: Part II: potential mechanisms. Circulation *105*, 1861–1870.

Zeng, L., Wu, G.Z., Goh, K.J., Lee, Y.M., Ng, C.C., You, A.B., Wang, J., Jia, D., Hao, A., Yu, Q., and Li, B. (2008). Saturated fatty acids modulate cell response to DNA damage: implication for their role in tumorigenesis. PLoS ONE *3*, e2329.

A Crucial Role of Activin A-Mediated Growth Hormone Suppression in Mouse and Human Heart Failure

Noritoshi Fukushima[1,2☯], Katsuhisa Matsuura[1,3*☯], Hiroshi Akazawa[4☯], Atsushi Honda[1], Toshio Nagai[5], Toshinao Takahashi[5], Akiko Seki[1], Kagari M. Murasaki[1], Tatsuya Shimizu[3], Teruo Okano[3], Nobuhisa Hagiwara[1,2], Issei Komuro[4*]

1 Department of Cardiology, Tokyo Women's Medical University, Tokyo, Japan, **2** Global Centers of Excellence (GCOE) Program, Tokyo Women's Medical University, Tokyo, Japan, **3** Institute of Advanced Biomedical Engineering and Science, Tokyo Women's Medical University, Tokyo, Japan, **4** Department of Cardiovascular Medicine, Osaka University Graduate School of Medicine, Osaka, Japan, **5** Department of Cardiovascular Science and Medicine, Chiba University Graduate School of Medicine, Chiba, Japan

Abstract

Infusion of bone marrow-derived mononuclear cells (BMMNC) has been reported to ameliorate cardiac dysfunction after acute myocardial infarction. In this study, we investigated whether infusion of BMMNC is also effective for non-ischemic heart failure model mice and the underlying mechanisms. Intravenous infusion of BMMNC showed transient cardioprotective effects on animal models with dilated cardiomyopathy (DCM) without their engraftment in heart, suggesting that BMMNC infusion improves cardiac function *via* humoral factors rather than their differentiation into cardiomyocytes. Using conditioned media from sorted BMMNC, we found that the cardioprotective effects were mediated by growth hormone (GH) secreted from myeloid (Gr-1(+)) cells and the effects was partially mediated by signal transducer and activator of transcription 3 in cardiomyocytes. On the other hand, the GH expression in Gr-1(+) cells was significantly downregulated in DCM mice compared with that in healthy control, suggesting that the environmental cue in heart failure might suppress the Gr-1(+) cells function. Activin A was upregulated in the serum of DCM models and induced downregulation of GH levels in Gr-1(+) cells and serum. Furthermore, humoral factors upregulated in heart failure including angiotensin II upregulated activin A in peripheral blood mononuclear cells (PBMNC) via activation of NFκB. Similarly, serum activin A levels were also significantly higher in DCM patients with heart failure than in healthy subjects and the GH levels in conditioned medium from PBMNC of DCM patients were lower than that in healthy subjects. Inhibition of activin A increased serum GH levels and improved cardiac function of DCM model mice. These results suggest that activin A causes heart failure by suppressing GH activity and that inhibition of activin A might become a novel strategy for the treatment of heart failure.

Citation: Fukushima N, Matsuura K, Akazawa H, Honda A, Nagai T, et al. (2011) A Crucial Role of Activin A-Mediated Growth Hormone Suppression in Mouse and Human Heart Failure. PLoS ONE 6(12): e27901. doi:10.1371/journal.pone.0027901

Editor: Piero Anversa, Brigham and Women's Hospital, United States of America

Received August 21, 2011; **Accepted** October 27, 2011; **Published** December 28, 2011

Funding: This study was supported by: The Global Centers of Excellence (COE) Program, Multidisciplinary Education and Research Center for Regenerative Medicine (MERCREM), from the Japanese Ministry of Education, Culture, Sports, Science and Technology (to N. Fukushima); a Grant-in-Aid for Scientific Research, Developmental Scientific Research, and Scientific Research from the Japanese Ministry of Education, Culture, Sports, Science and Technology; Uehara Memorial Research Grant (to KM); Grants from the Japanese Ministry of Education, Culture, Sports, Science and Culture and Health and Labor Sciences Research Grants (to HA); and a Grant-in-Aid for Scientific Research on Priority Areas and for Exploratory Research from the Japanese Ministry of Education, Culture, Sports, Science and Technology (to IK). The funders had no role in study design, data collection and analysis, decision to publish, or preparation of the manuscript.

Competing Interests: The authors have declared that no competing interests exist.

* E-mail: kmatsuura@abmes.twmu.ac.jp (KM); komuro-tky@umin.ac.jp (IK)

☯ These authors contributed equally to this work.

Introduction

Heart failure is a major cause of mortality in many countries. Infusion of bone marrow-derived mononuclear cells (BMMNC) is expected as a novel treatment of heart failure. Animal experiments and clinical trials have shown that BMMNC infusion ameliorates cardiac dysfunction after acute myocardial infarction and chronic myocardial ischemia [1]–[4]. Although the outcomes vary among trials, recent meta-analyses revealed that cardiac function slightly improves following BMMNC infusion for ischemic heart diseases [5], [6]. Bone marrow cells were reported to be incorporated into the damaged myocardium and to differentiate into various cell types including cardiomyocytes [7]. However, whether bone marrow-derived stem cells can differentiate into many cardiomyocytes is still an open question [8]. There are many reports indicating that transplantation of various types of stem cells improves the cardiac function of ischemic hearts, mainly by paracrine factors which induce angiogenesis and cardioprotection [9]–[11]. Since the effects of BMMNC infusion for non-ischemic cardiomyopathy remain unknown, we examined whether BMMNC infusion also improves cardiac function of non-ischemic cardiomyopathy.

Results

Preparation of non-ischemic dilated cardiomyopathy (DCM) mice

Two kinds of non-ischemic DCM mice were used. The first model was generated by transgenic overexpression of a mutant epidermal growth factor receptor (EGFR) with C-terminal truncation (EGFRdn). The expression of mutant EGFRdn is